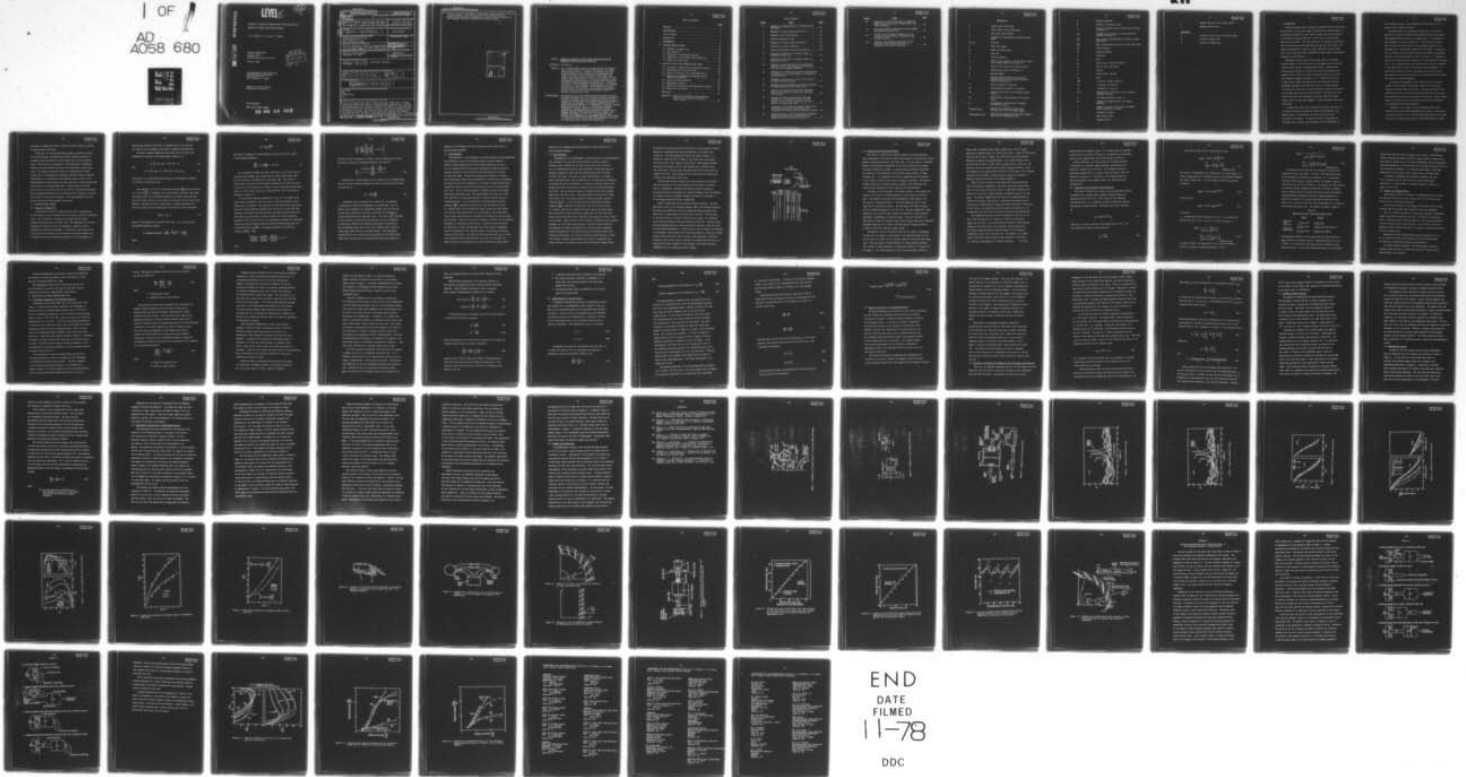


AD-A058 680

PENNSYLVANIA STATE UNIV UNIVERSITY PARK APPLIED RESE--ETC F/G 20/4  
STUDIES OF A METHOD TO PREVENT DRAFT TUBE SURGE AND THE ANALYSI--ETC(U)  
MAR 78 W S GEARHART, A M YOCUM, T SEYBERT N00017-73-C-1418  
TM-78-56

UNCLASSIFIED

1 OF 1  
AD  
A058 680



END  
DATE  
FILMED  
11-78  
DDC

AD A0 58680

DDC FILE COPY

LEVEL II

12  
R

STUDIES OF A METHOD TO PREVENT DRAFT TUBE SURGE AND THE  
ANALYSIS OF WICKET GATE FLOW AND FORCES

W. S. Gearhart, A. M. Yocum, T. Seybert

Technical Memorandum  
File No. 78-56  
20 March 1978  
Contract No. N00017-73-C-1418 ✓

Copy No. 24

DDC  
RECEIVED  
SEP 15 1978  
F

The Pennsylvania State University  
APPLIED RESEARCH LABORATORY ✓  
Post Office Box 30  
State College, PA 16801

Approved for Public Release  
Distribution Unlimited

NAVY DEPARTMENT

NAVAL SEA SYSTEMS COMMAND

78 09 14 055

UNCLASSIFIED

SECURITY CLASSIFICATION OF THIS PAGE (When Data Entered)

REPORT DOCUMENTATION PAGE		READ INSTRUCTIONS BEFORE COMPLETING FORM
1. REPORT NUMBER TM-78-56	2. GOVT ACCESSION NO.	3. RECIPIENT'S CATALOG NUMBER
4. TITLE (and Subtitle) STUDIES OF A METHOD TO PREVENT DRAFT TUBE SURGE AND THE ANALYSIS OF WICKET GATE FLOW AND FORCES		5. TYPE OF REPORT & PERIOD COVERED Technical Memorandum
7. AUTHOR(s) W. S. Gearhart, A. M. Yocum, T. Seybert		6. PERFORMING ORG. REPORT NUMBER
9. PERFORMING ORGANIZATION NAME AND ADDRESS Applied Research Laboratory Post Office Box 30 State College, PA 16801		8. CONTRACT OR GRANT NUMBER(s) 6-07-DR-50160
11. CONTROLLING OFFICE NAME AND ADDRESS Bureau of Reclamation, Engr. and Research Center P. O. Box 25007, Bldg. 56, Denver Federal Center Denver, Colorado 80225		10. PROGRAM ELEMENT, PROJECT, TASK AREA & WORK UNIT NUMBERS
14. MONITORING AGENCY NAME & ADDRESS (if different from Controlling Office) Naval Sea Systems Command Washington, DC 20362		12. REPORT DATE 20 March 1978
		13. NUMBER OF PAGES 68
		15. SECURITY CLASS. (of this report) UNCLASSIFIED
		15a. DECLASSIFICATION/DOWNGRADING SCHEDULE
16. DISTRIBUTION STATEMENT (of this Report) Approved for public release. Distribution unlimited. Per NAVSEA - Aug. 28, 1978.		
17. DISTRIBUTION STATEMENT (of the abstract entered in Block 20, if different from Report) 9 Technical memos   12 74 p		
18. SUPPLEMENTARY NOTES 15 N00017-73-C-1418		
19. KEY WORDS (Continue on reverse side if necessary and identify by block number) draft tube surge turbomachinery flow		
20. ABSTRACT (Continue on reverse side if necessary and identify by block number) An air flow facility was used to simulate the flow through a set of wicket gates and the draft tube typical of a hydroelectric pump-turbine. A method of preventing draft tube surge was studied, which consists of injecting some high energy fluid from the spiral casing into the draft tube counter to the direction of the swirl. The results of these tests provide design criteria for selecting injection nozzle configuration and estimating the required injection flow for a turbine of given performance characteristics. A potential		

DD FORM 1 JAN 73 1473

78 09 14 055 EDITION OF NOV 65 IS OBSOLETE

UNCLASSIFIED

391 007 SECURITY CLASSIFICATION OF THIS PAGE (When Data Entered)

UNCLASSIFIED

SECURITY CLASSIFICATION OF THIS PAGE (When Data Entered)

20. solution of the flow through a two-dimensional radial cascade of airfoils is also presented. The predicted flow field characteristics are compared with experimental measurements, and the results indicate very good agreement between the measured and predicted values.

ACCESSION for		
NTIS	DTIC Section	<input checked="" type="checkbox"/>
DDC	DTIC Section	<input type="checkbox"/>
UNANNOUNCED		<input type="checkbox"/>
JUSTIFICATION		
BY		
DISTRIBUTION/AVAILABILITY CODES		
DI		CONFIDENTIAL
A		

UNCLASSIFIED

SECURITY CLASSIFICATION OF THIS PAGE (When Data Entered)

**Subject:** Studies of a Method to Prevent Draft Tube Surge and the Analysis of Wicket Gate Flow and Forces

**References:** See page 43.

**Abstract:** An air flow facility was used to simulate the flow through a set of wicket gates and the draft tube typical of a hydroelectric pump-turbine. A method of preventing draft tube surge was studied, which consists of injecting some high energy fluid from the spiral casing into the draft tube counter to the direction of the swirl. The results of these tests provide design criteria for selecting injection nozzle configuration and estimating the required injection flow for a turbine of given performance characteristics. A potential solution of the flow through a two-dimensional radial cascade of airfoils is also presented. The predicted flow field characteristics are compared with experimental measurements, and the results indicate very good agreement between the measured and predicted values.

**Acknowledgment:** The major portion of the technical work was sponsored by the United States Department of the Interior, Bureau of Reclamation of Denver, Colorado, as part of the Bureau's Pumped Storage Research Activities under their Energy Research and Development Program and the remainder of the work was sponsored by the Naval Sea Systems Command, U. S. Department of the Navy. Special thanks is given to Dr. Ing. H. T. Falvey of the Bureau of Reclamation at Denver, Colorado, who provided frequent consultation and implemented the exchange of information and hardware required in the completion of this program. The guidance and comments of Dr. G. F. Wislicenus were most helpful in the conceptual and development phases of this effort. F. Archibald's efforts in providing instrumentation to obtain the unsteady pressure spectra were appreciated.

Table of Contents

	<u>Page</u>
Abstract . . . . .	1
Acknowledgment . . . . .	1
List of Figures . . . . .	3
Nomenclature . . . . .	5
1. INTRODUCTION . . . . .	8
2. INJECTION NOZZLE STUDIES . . . . .	10
2.1 Estimate of Bypass Flow . . . . .	10
2.2 Test Apparatus . . . . .	14
2.3 Discussion of Experimental Results . . . . .	17
2.4 Comparison of Test Results with Predictions . . . . .	19
2.5 Summary and Conclusions . . . . .	22
3. ANALYSIS OF FLOW FIELD THROUGH WICKET GATES . . . . .	23
3.1 Preliminary Assumptions and Governing Equations . . . . .	23
3.2 Transformation of the Flow Field . . . . .	28
3.3 Method of Solution in the Transformed Plane . . . . .	31
3.4 Discussion of Normalizing Parameters and the Reverse Transformation . . . . .	32
3.5 Analytical Study Conducted . . . . .	35
3.6 Experimental Program . . . . .	36
3.7 Discussion of Analytical and Experimental Results . . . . .	38
3.8 Summary and Conclusions . . . . .	42
References . . . . .	43
Appendix A - Results of Preliminary Tests Indicating Effect of Test Apparatus Geometry on Surge Pressure . . . . .	61

List of Figures

<u>Figure</u>	<u>Title</u>	<u>Page</u>
1	Schematic of Proposed Means of Preventing Draft Tube Surge . . . . .	44
2	Schematic of Flow Leaving Wicket Gates . . . . .	45
3	Schematic of Air Flow Facility . . . . .	46
4	Spectral Analysis of Surge . . . . .	47
5	Comparison of Nozzle Angle of Injection . . . . .	48
6	Comparison of Nozzle Geometries . . . . .	49
7	Axial and Tangential Velocity Distribution . . . . .	50
8	Injected Flow Required to Eliminate Surge for Cylindrical Draft Tube . . . . .	51
9	Injected Flow Required to Eliminate Surge for Elbow Draft Tube . . . . .	52
10	Schematic of Two Wicket Gates Illustrating the Graphical Method of Determining the Flow Angle and, hence, the Momentum Parameter . . . . .	53
11	Schematic of a Turbine Cross Section Illustrating the Geometry of the Flow Passage in the Region of the Wicket Gates . . . . .	54
12	Schematic of a Sector of a Wicket Gate System in the Real Coordinate System . . . . .	55
13	Schematic of the Two-Dimensional Cascade Obtained by Transforming the Wicket Gate System . . . . .	55
14	Sketch of the Wicket Gate and Draft Tube Model Used to Experimentally Evaluate the Potential Flow Solution . . . . .	56
15	Average Flow Angle versus Wicket Gate Angle Obtained for the Symmetrical Gates from the Potential Flow Solution, Graphical Prediction Method, and Experimental Data . . . . .	57
16	Comparison of the Fluid Exit Angles Predicted for the Cambered Wicket Gate System Using the Potential Flow Solution and the Graphical Approach .	58
17	Local Fluid Angle versus Circumferential Location Measured Downstream of the Wicket Gates and Predicted by the Potential Flow Solution . . . . .	59

<u>Figure</u>	<u>Title</u>	<u>Page</u>
18	Schematic of a Wicket Gate and the Cascade of Wicket Gates Describing the Program Input and Output Parameters . . . . .	60
A.1	Axial and Tangential Velocities in the Original and Modified Test Facility . . . . .	66
A.2	Pressure versus Momentum Parameter for the Cylindrical Draft Tube as a Function of Test Facility Geometry . . . . .	67
A.3	Pressure versus Momentum Parameter for the Fontenelle (Elbow Type) Draft Tube as a Function of Test Facility Geometry . . . . .	68

Nomenclature

B	depth of the wicket gates
c	chord length of the wicket gates
D	draft tube inlet diameter
f	frequency of the pressure pulsations during surge
$F_1, F_2$	functions
L	draft tube length
N	number of wicket gates
Q	flow rate
r	radial coordinate
$r_1$	radius to the center of the exit from a wicket gate passage (defined by Figure 10)
$r_s$	radius of the wicket gate spindle centers
R	dimensionless radial coordinate, $r/c$
Re	Reynolds number
s	minimum spacing between one wicket gate trailing edge and the adjacent wicket gate (defined by Figure 10)
$v_r$	radial component of velocity
$v_\theta$	circumferential component of velocity
$v_{r_s}$	normalizing velocity in the original plane = $Q/2\pi Br_s$
$V_R$	dimensionless radial component of velocity, $v_r/v_{r_s}$
$V_\theta$	dimensionless circumferential component of velocity, $v_\theta/v_{r_s}$
$V_{\text{original plane}}$	dimensionless magnitude of the total velocity vector in the original plane
$V_{\text{transformed plane}}$	dimensionless magnitude of the total velocity vector in the transformed plane

S	momentum parameter
D'	diameter of injection nozzle
$r_i$	radius of trailing edge of wicket gates (defined by Figure 2)
$v_{\theta i}$	circumferential velocity at wicket gate exit (defined by Figure 2)
$\overline{v_{\theta T}}$	mass averaged circumferential velocity in draft tube throat
$\overline{v_{AT}}$	mass averaged axial velocity in draft tube throat
$Q_B$	bleed discharge
$Q_T$	turbine discharge
$\eta$	efficiency
H	head
$A_N$	total area of injection nozzles
$A_T$	area of draft tube throat
$\gamma$	density
g	gravitational constant
P	power
$\sqrt{P^2}$	rms value of surge condition
$v_x$	x component of velocity
$v_y$	y component of velocity
X, Y	dimensionless coordinates of the cartesian coordinate systems
$\alpha$	flow angle defined by Figure 10
$\overline{\alpha}$	average flow angle based on the angular momentum
$\theta$	angular coordinate in the polar coordinate system expressed in radians
$\nu$	kinematic viscosity
$\rho$	mass density ( $\gamma/g$ )
$\psi$	stream function

$\omega$  angular velocity of the turbine runner  
 $\Omega$  angular momentum flux

SUBSCRIPTS

i evaluated at the exit of the wicket gates  
B related to bypass flow  
T related to turbine flow

## 1. INTRODUCTION

A study was undertaken to evaluate a proposed method of preventing the occurrence of draft tube surge in hydroelectric pump-turbines. It is generally accepted that the origin of draft tube surge is related to the amount of angular momentum or swirl left in the discharge flow from the turbine. The swirl gives rise to unstable flow patterns which causes pressure pulsations described as draft tube surge. The adverse consequences of surge are noise, vibration, vertical movement of the runner and shaft, variations in power output, and pressure pulsations in the penstock.

Realizing that the onset of draft tube surge is associated with the amount of swirl present in the discharge flow, the obvious solution would consist of eliminating the swirl. Straightening vanes and fins located in the draft tube have been suggested and tried, but have resulted in either efficiency losses or structural and cavitation damage as reported in [1]. Injection of air has, in some cases, reduced the magnitude of the pressure pulsations. Appendages attached in the draft tube such as a hollow cylinder to contain the vortex core or solid fairings to reduce the intensity of the vortex have met with limited success. The majority of the methods that have been attempted cause either excessive energy losses, result in cavitation damage, or induce excessive structural vibrations.

A method that reduces the rotation in the draft tube flow at off-design conditions and does not effect the efficiency of the machine when it is operating at or near its point of best efficiency is necessary. It must not consist of appendages in the draft tube or impair the performance of the machine when it

is operating as a pump. The elimination of either positive or negative swirl should be provided.

The method that is considered and evaluated in this report consists of a series of flush mounted nozzles located in the draft tube immediately downstream of the turbine rotor. A schematic of the arrangement is shown in Figure (1). The nozzles will inject fluid in the draft tube counter to the peripheral motion of the discharge flow. Although not indicated in the figure, two separate rows of nozzles could be provided with one row capable of injecting fluid in a direction opposite to that of the other. An arrangement such as this would permit the reduction of either positive or negative swirl. It is envisioned that the nozzles will be directly connected to the high pressure fluid in the spiral casing or penstock. An appropriate system of valving, activated on the basis of wicket gate opening, would control the flow to the nozzles and could control the number of nozzles discharging.

An alternate arrangement to that shown in Figure (1) would consist of swirl nozzles individually connected to the spiral casing by separate piping and valving. The nozzles would be flush mounted on the wall of the draft tube and thereby provide a minimum flow disturbance when the swirl nozzles are inactive. Their presence should not cause any loss in efficiency or cavitation resistance of the machine when they are inactive.

Contained in this report is an experimental study of the efficiency of various nozzle geometries with respect to the removal of swirl in the draft tube. The resulting empirical data is applied to specific turbine applications to illustrate a method to predict

the amount of bypass fluid and to specify the nozzle geometry required to suppress draft tube surge.

In addition to the injection nozzle studies a potential solution of the flow through a two-dimensional radial cascade of airfoils is presented, where the airfoils in the cascade can be of any arbitrary shape. This solution is applicable to the wicket gates of hydraulic turbines and was developed as an aid in the prediction of draft tube surge. The method of solution consists of transforming the radial cascade into a two-dimensional rectangular cascade by using a conformal transformation. An existing cascade analysis program, known as the Douglas-Neumann Cascade Program, was then employed to obtain the potential flow solution in the transformed plane. Using a model of a wicket gate and draft tube system, with air as the fluid, experiments measuring the flow angles downstream of the wicket gates were conducted to evaluate the accuracy of the prediction method. Very good agreement was found between the measured and predicted fluid angles.

## 2. INJECTION NOZZLE STUDIES

### 2.1 Estimate of Bypass Flow

A theoretical estimate of required bypass flow to implement the proposed means of surge elimination shown in Figure 1 shall be established first. This fluid shall be assumed to be piped from the spiral casing and discharged into the draft tube. The bypassing of such fluid represents an energy loss that, for purposes of analysis, will be considered as totally unrecoverable. On this basis, the swirl in the draft tube must be reduced to some specified value with a minimum rate of injected fluid if the described technique is to be successful. An

engineering estimate of the ratio of bypassed flow to flow through the turbine can be obtained on the basis of momentum considerations.

The flux of angular momentum ( $\Omega$ ) and draft tube flow ( $Q$ ) can be determined at the exit of the wicket gates, Figure 2, as:

$$Q = \int V \cos \alpha \, dA = V \cos \alpha \, 2\pi r B \quad (1)$$

and

$$\Omega = \rho \int V \cos \alpha (r V \sin \alpha) \, dA = \rho Q r_1 V_{\theta_1} \quad (2)$$

The quantity  $B$  is wicket gate depth and  $V_{\theta_1}$  is the peripheral component of velocity at wicket gate exit.

From equations (1) and (2) the momentum parameter  $\frac{\Omega D}{\rho Q^2}$  can be converted to a ratio of  $\frac{V_{\theta T}}{V_{AT}}$  by assuming a free vortex flow in the draft tube, where the quantity  $V_{\theta T}$  is the peripheral velocity at the draft tube wall, and  $V_{AT}$  is the axial velocity at the entrance to the draft tube (or exit of the turbine). Applying the law of conservation of angular momentum to the flow as it passes from the wicket gates and enters the draft tube gives:

$$\frac{D}{2} V_{\theta T} = V_{\theta_1} r_1 \quad (3)$$

where  $D$  is the diameter of the draft tube inlet. By (1), (2) and (3), the momentum parameter becomes:

$$S = \text{Momentum Parameter} = \frac{\Omega D}{\rho Q^2} = \frac{V_{\theta_1} r_1 D}{Q} = \frac{2 V_{\theta T}}{\pi V_{AT}}$$

where

$$Q = (V_{AT}) \left( \frac{\pi D^2}{4} \right) .$$

The ratio of peripheral to axial velocity can now be written in terms of the momentum parameter:

$$\frac{V_{\theta T}}{V_{AT}} = 1.57 \left( \frac{\Omega D}{\rho Q^2} \right) = 1.57 (S) . \quad (4)$$

It is proposed to reduce the swirl that exists in the draft tube at any given gate opening,  $V_{\theta T}$ , to that level of swirl which exists prior to the occurrence of periodic draft tube surge,  $V_{\theta T}^*$ . This level of swirl would be attained when the angular momentum of the draft tube flow and that of the injected fluid is summed to give a resultant momentum parameter,  $S$ , which is less than that at which periodic draft tube surge is predicted to occur,  $S^*$ .

If the critical momentum parameter  $S^*$  is not to be exceeded in the draft tube, the amount of fluid that must be injected through the swirl nozzles can be evaluated. The quantities of flow and velocity associated with the critical momentum parameter shall be noted by an asterisk, and subscript (T) denotes flow and velocities associated with the draft tube. The quantity of bleed fluid required to obtain the critical momentum parameter  $S^*$  in the draft tube can be determined by equating the difference between the angular momentum from the turbine discharge  $Q_T r V_{\theta T}$  and that of the bleed fluid  $Q_B r \sqrt{2gH}$  to the angular momentum at the critical condition  $Q_T^* r V_{\theta T}^*$ . Thus,

$$\frac{(Q_T r V_{\theta T})}{(Q_T^* r V_{AT}^*)} - \frac{Q_B r \sqrt{2gH}}{(Q_T^* r V_{AT}^*)} = \left( \frac{Q_T^* r V_{\theta T}^*}{Q_T^* r V_{AT}^*} \right) = 1.57 S^*$$

and

$$\frac{Q_B}{Q_T^*} = \frac{V_{AT}^*}{\sqrt{2gH}} \left\{ \left[ \frac{Q_T v_{\theta T}}{Q_T^* V_{AT}^*} - 1.57 S^* \right] \right\} .$$

The above can be rearranged to provide a ratio of bypass flow to draft tube flow in terms of the momentum parameters (S) and (S<sup>\*</sup>):

$$\frac{Q_B}{Q_T} = \frac{1.57 V_{AT}^* \left[ S \left( \frac{V_{AT}}{V_{AT}^*} \right) - \left( \frac{V_{AT}}{V_{AT}^*} \right) S^* \right]}{\sqrt{2gH}} \quad (5)$$

The decrease in efficiency ( $\Delta\eta$ ) of the turbine due to bleeding bypass fluid to the swirl nozzles assuming that none of the bypass fluid energy is recovered is:

$$\Delta\eta = (100) \left( \frac{Q_B}{Q_T} \right) \quad (6)$$

If Equation (5) is considered for a given (S), the numerator is essentially constant and independent of turbine head. This is based on the assumption, for cavitation purposes, that the velocity at the design condition in the draft tube throat for conventional turbine installations has some upper limit. The ratio of  $\frac{Q_B}{Q_T}$  specified by (5) decreases as some reciprocal function as head is increased. On this basis, Equation (6) indicates the decrease in efficiency, due to bleeding bypass fluid to the swirl nozzles, will be less in a high head turbine than in a low head turbine. The performance characteristics for a turbine such as presented for the Grand Coulee Third Power Plant Units in [3] provides the quantities required in

equation (5) to estimate the ratio of bypass to draft tube flow at a given momentum parameter.

## 2.2 Test Apparatus

Investigations of the performance of various injection nozzle geometries were conducted in an air flow facility which is shown in Figure 3. Similar studies conducted in [2] and [4] have shown that the use of air as a working fluid has been quite successful in characterizing the momentum parameter in draft tube flow and predicting the occurrence of draft tube surge. The main air supply was provided by a variable speed centrifugal blower and was measured by an orifice meter arrangement. The metered air flow was diffused as it entered a stilling chamber where screens were used to reduce flow turbulence across the stilling chamber flow field. The air radially entered a cylindrical draft tube through wicket gate type swirl vanes. The angle between the vanes and a radial line could be set at any angle between 0° (radial position) and 82.5° (closed position). It can be shown that the dimensionless momentum parameter,  $\frac{\Omega D}{\rho Q^2}$ , reduces to  $K (\tan \bar{\alpha})$  for this test facility, where  $K = \text{constant}$  and  $\bar{\alpha}$  is the average flow angle leaving the wicket gates. Flow traverse data taken across the trailing edge of the wicket gates using a prism probe were used to determine flow angles for various wicket gate settings. These data were used to develop a relation for the momentum parameter as a function of gate setting. Injection fluid provided by an auxiliary air supply and measured by an orifice meter arrangement, entered the manifold of the injection nozzle test section located just below the wicket gates. Any ratio of injection fluid flow,  $Q_B$ , to fluid flow through the gates (turbine flow),  $Q_T$ , could be provided by the proper setting of a butterfly valve on the auxiliary air supply blower.

equation (5) to estimate the ratio of bypass to draft tube flow at a given momentum parameter.

## 2.2 Test Apparatus

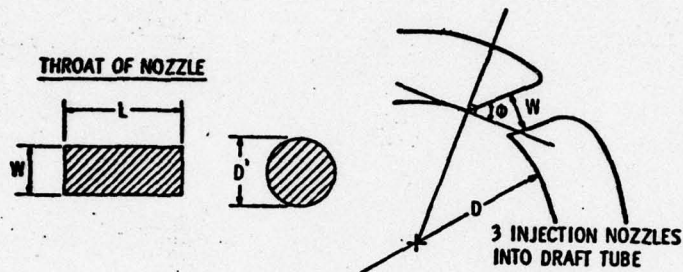
Investigations of the performance of various injection nozzle geometries were conducted in an air flow facility which is shown in Figure 3. Similar studies conducted in [2] and [4] have shown that the use of air as a working fluid has been quite successful in characterizing the momentum parameter in draft tube flow and predicting the occurrence of draft tube surge. The main air supply was provided by a variable speed centrifugal blower and was measured by an orifice meter arrangement. The metered air flow was diffused as it entered a stilling chamber where screens were used to reduce flow turbulence across the stilling chamber flow field. The air radially entered a cylindrical draft tube through wicket gate type swirl vanes. The angle between the vanes and a radial line could be set at any angle between 0° (radial position) and 82.5° (closed position). It can be shown that the dimensionless momentum parameter,  $\frac{\Omega D}{\rho Q^2}$ , reduces to  $K (\tan \bar{\alpha})$  for this test facility, where  $K = \text{constant}$  and  $\bar{\alpha}$  is the average flow angle leaving the wicket gates. Flow traverse data taken across the trailing edge of the wicket gates using a prism probe were used to determine flow angles for various wicket gate settings. These data were used to develop a relation for the momentum parameter as a function of gate setting. Injection fluid provided by an auxiliary air supply and measured by an orifice meter arrangement, entered the manifold of the injection nozzle test section located just below the wicket gates. Any ratio of injection fluid flow,  $Q_B$ , to fluid flow through the gates (turbine flow),  $Q_T$ , could be provided by the proper setting of a butterfly valve on the auxiliary air supply blower.

The nozzle test section provided three points of fluid injection equally spaced in a circumferential plane perpendicular to the draft tube centerline. The nozzle geometries tested are shown in Table I. It should be pointed out that in Table I,  $A_N$ , nozzle area, was defined as the sum of the three separate nozzle areas. After passing through the nozzle test section, the air flow entered the cylindrical draft tube ( $L/D=4.56$ ). Pressure taps and probe holes were located along the length of the tube. The cylindrical draft tube could be replaced with an elbow type (Fontenelle) draft tube.

The unsteady pressure produced by the swirling flow in the draft tube was monitored at the last pressure tap ( $L/D=4.40$ ) on the draft tube by a dynamically calibrated differential pressure transducer. The pressure signal was analyzed by a Spectral-Dynamics real time analyzer in conjunction with an ensemble averager from which the frequency,  $f$ , of the surging condition could be established.

Figure 4 shows typical data obtained from the analyzer. The root-mean-square value of the unsteady pressure,  $\sqrt{p^2}$ , at the surging condition was read from an RMS meter after the signal was passed through a line filter with a characteristic 48 dB per octave roll-off. The band pass of the filter was set at 20 Hz to 120 Hz for all tests. The frequency of all observed pressure surges was between 35 and 70 Hz. Directly across from the pressure pickup tap used on the draft tube was a probe hole used for flow field measurements. A prism probe was used to obtain the time-mean total pressure, static pressure and fluid flow angle as a function of radial distance across the draft tube for various flow conditions. The basic parameters used in this study to describe the surging condition were the dimensionless groups suggested by [5]; namely, the pressure parameter  $(D^4 \sqrt{p^2} / \rho Q^2)$  and the frequency parameter  $(fD^3/Q)$ .

Table I  
NOZZLE SHAPES TESTED



Nozzle Number	Injection Angle, $\phi$ (deg)	Nozzle Area, $A_N$ (sq in.)	$A_N/A_T$ (%)	L/W
1	30	1.500	5.09	8.0
2	↓	0.750	2.54	4.0
3	↓	0.375	1.27	0.5
4	↓	1.125	3.84	1.5
5	0	0.750	2.54	1.0
	15	↓	↓	↓
	30	↓	↓	↓
	45	↓	↓	↓
6	30	0.188	0.64	4.0
7	↓	0.750	2.54	0.25
8	↓	0.610	2.04	circle, $D' = 0.5$ in.
9	↓	1.325	4.48	circle, $D' = 0.75$ in.
10	↓	0.375	1.27	1.0
11	↓	↓	↓	4.0
12	↓	↓	↓	0.25
13	↓	1.50	5.04	1.0
14	↓	↓	↓	4.0
15	↓	↓	↓	0.25

### 2.3 Discussion of Experimental Results

The effect of various fluid injection angles and nozzle geometries were investigated on the basis of their effectiveness in reducing the unsteady pressure amplitude measured in the draft tube. All tests were at a Reynolds Numbers above 80,000 as recommended in [4] and at velocities low enough to prevent compressible effects. A typical spectral analysis indicating the reduction in the amplitude of the unsteady surge pressure is shown by Figure (4). It is apparent that both the amplitude and the frequency of the surge are reduced as the ratio of  $Q_B/Q_T$  is increased. The spectral analysis indicates no pressure peaks at a  $Q_B/Q_T$  of 16% indicating that surge has been eliminated at this condition of fluid injection.

The angle of fluid injection, as defined in Table I, was studied with respect to its effect on reducing surge for a given swirl in the draft tube. Four angles of injection were investigated, these being  $0^\circ$ ,  $15^\circ$ ,  $30^\circ$  and  $45^\circ$  as defined by Table I. The nozzle geometry used in these tests was #5, described in Table I, and the results are shown in Figure (5) for a momentum parameter of 0.8 and 1.18. The most significant result being that, up to the  $45^\circ$  angle tested, the reduction of surge pressure amplitude is independent of injection angle. The lower end points of the curves in Figure (5) represent that ratio of  $Q_B/Q_T$  required to completely eliminate surge and it is evident that the quantity of  $Q_B/Q_T$  required, is equal for the four injection angles tested.

An injection angle of  $30^\circ$  was selected for the tests to investigate the effect of the length to width ratio of the injection nozzle as well as the ratio of the area of the injection nozzles to the draft tube throat area. The ratio  $Q_B/Q_T$  is plotted against the surge pressure parameter for a series of nozzle geometries for momentum parameters of 0.8 and 1.18 in Figure 6. The lower extremity of each curve represents a condition

where surge is eliminated and thereby indicates the ratio of  $Q_B/Q_T$  required to eliminate surge for a given  $A_N/A_T$  ratio. Figure (6) illustrates that for a given ratio of  $Q_B/Q_T$ , the reduction in the surge pressure amplitude is greater as  $A_N/A_T$  decreases. This results directly from the fact that to inject a given ratio of  $Q_B/Q_T$  into the draft tube, the head and, hence, the velocity must increase as  $A_N/A_T$  decreases. Since the momentum of the injected fluid increases as the square of the spouting velocity from the nozzles, smaller ratios of  $Q_B/Q_T$  are required to eliminate surge as the head on the turbine increases.

Table I lists the various nozzle geometries tested and defines their characteristic dimensions. The rather surprising result being that for the various L/W nozzles tested, no measurable difference was observed in the ratio of  $Q_B/Q_T$  required to eliminate surge at a given  $A_N/A_T$ . This result suggests that the choice of a nozzle geometry to obtain a given  $A_N/A_T$  would consist of selecting that geometry which would give the least hydraulic losses and permit the easiest fabrication. On this basis, a cylindrical nozzle which would be elliptical at its intersection with the barrel of the draft tube would seem appropriate.

The tangential and axial velocity components of the flow in the draft tube were measured at a station of  $L/D=4.40$ , indicated on Figure (3), by means of a prism probe which provided a time-averaged reading of the local static, total pressure and flow angularity. The velocity distributions are shown by Figure (7) for momentum parameters of 0.24, 0.41, 0.80 and 1.18. The dashed line in these figures represents similar traverse data having the wicket gates at a setting corresponding to a momentum parameter of 0.8 but with

fluid injected to eliminate surge. It is evident that the reversal of axial flow at the axis of rotation is eliminated and considerable swirl has been removed from the flow when fluid is injected.

Without injection, the outer portion of the flow approaches a free vortex, or constant angular momentum, distribution with solid body rotation near the center. The peripheral velocity distribution downstream of a turbine runner may deviate from that indicated in Figure (7). The effect of such variation has not been investigated in the present studies, but deserves future consideration.

#### 2.4 Comparison of Test Results with Predictions

The ratio of bleed flow to turbine flow was previously derived in Equation (5), assuming ideal momentum transfer between the injected and draft tube flow. On the basis of the preceding experimental data, it is possible to obtain an empirical relation that applies to pump-turbines. The bypass flow can be expressed as

$$Q_B = K_1 (2g H)^{1/2} A_N \quad , \quad (7)$$

where  $K_1$  is a nozzle coefficient and assumed equal to 0.9. The flow through the turbine can be written as

$$Q_T = \frac{1}{\eta} \frac{P}{H\gamma} \quad . \quad (8)$$

The ratio of bleed flow to turbine flow is then

$$Q_B/Q_T = 39,100 \eta \frac{A_T}{P} \frac{A_N}{A_T} H^{3/2}$$

$$= \left[ (451 \eta \frac{A_T}{P} \frac{A_N}{A_T} H^{3/2}) \right] \text{English Units} \quad . \quad (9)$$

The results of experimental data indicating, for a given  $A_N/A_T$ , the ratio of  $Q_B/Q_T$  required to eliminate surge at two momentum parameters are shown in Figure (8). A curve fitting of this data indicates a relation

$$Q_B/Q_T = 0.719 (A_N/A_T)^{0.401} \quad (10)$$

for  $S=1.18$  and,

$$Q_B/Q_T = 0.473 (A_N/A_T)^{0.366} \quad (11)$$

for  $S=0.80$ .

Considering a momentum parameter of 1.18, it is possible by substituting (10) in (9) to obtain a relation for  $Q_B/Q_T$  of,

$$Q_B/Q_T = \frac{1}{2054 \left[ (\eta) \frac{A_T}{P} \right]^{0.67} H}$$

$$= \left[ \frac{1}{104.7 \left[ (\eta) \frac{A_T}{P} \right]^{0.67} H} \right] \text{English Units} \quad . \quad (12)$$

In similar fashion, the substitution of (11) in (9) provides a relation of  $Q_B/Q_T$  for a momentum parameter of 0.8,

$$Q_B/Q_T = \frac{1}{1460 \left(\frac{\eta A_T}{P}\right)^{0.578} H^{0.867}}$$

$$= \left( \frac{1}{111.5 \left(\frac{\eta A_T}{P}\right)^{0.578} H^{0.867}} \right) \text{ English Units} \quad . (13)$$

An elbow-type draft tube was also evaluated to indicate the influence of draft tube shape. The draft tube tested was similar to the Fontonelle configuration described in [4]. The data and equations relating  $A_N/A_T$  to  $Q_B/Q_T$  required to eliminate surge for this draft tube are shown in Figure 9. By applying the same analysis as indicated for the cylindrical draft tube, the ratio of bypass flow to turbine flow for the elbow-type draft tube was calculated. Using performance, geometrical data and a speed coefficient of  $\phi=0.8$  for the model of the Grand Coulee Third Power Plant Units given in [3], the bypass flow rates were determined for a cylindrical, and an elbow-type draft tube. The results are shown in Table II.

Table II

GRAND COULEE THIRD POWER PLANT BYPASS RATES

	<u>S=0.8</u>	<u>S=1.18</u>
Predicted Ideal (Eq. (5))	$Q_B/Q_T=4.49\%$	$Q_B/Q_T=3.97\%$
Predicted Empirically	$Q_B/Q_T=10.3\%$	$Q_B/Q_T=13.9\%$ (cylindrical)
	$Q_B/Q_T=11.5\%$	$Q_B/Q_T=13.0\%$ (elbow)

The comparison indicates that the empirically derived quantity of  $Q_B/Q_T$  required to eliminate surge at a momentum parameter of 1.18 is about 3.5 times greater than that predicted assuming an ideal momentum transfer. At the lower momentum parameter, the difference

between the estimated values of  $Q_B/Q_T$  is not as great. The difference between predicted and measured values of  $Q_B/Q_T$  required to prevent draft tube surge is primary due to the initial assumptions that the peripheral velocity distribution in the draft tube was a potential vortex and that the axial velocity was uniform. It is apparent from Figure 7 that these assumptions are not realistic when surge occurs in the draft tube.

It should be emphasized that solution of Equation (12) and (13) in conjunction with Figure (8) also specifies the  $A_N/A_T$  required, for a given turbine, to eliminate surge at a value of  $S$  equal to 0.8 or 1.18.

## 2.5 Summary and Recommendations

Experimental studies with respect to eliminating draft tube surge by injecting fluid into the draft tube counter to the existing swirl resulted in the following observations.

As the ratio of injected fluid  $Q_B/Q_T$  is increased, both the surge frequency and the unsteady surge pressure decreases in magnitude.

The use of various nozzles of a fixed  $A_N/A_T$  indicates no measurable change in the effectiveness of the nozzle in reducing or eliminating surge. Similarly, nozzle injection angles up to  $45^\circ$  show no difference in their effectiveness in reducing surge. On this basis, the nozzle geometry would be selected primarily on the basis of hydraulic efficiency and ease of fabrication.

Empirical data are presented which permits estimating the area of the injection nozzles and the quantity of bleed fluid required for turbines of specified performance characteristics.

At a given momentum parameter, the quantity  $Q_B/Q_T$  required to eliminate surge decreases as higher head turbines or lower specific speed machines are considered.

Further investigations are required to gather data indicating the influence of draft tube shape on the effectiveness of fluid injection in reducing draft tube surge.

The hydrodynamic effects such as cavitation arising from the interaction of the draft tube flow with the high velocity injection jets should be experimentally investigated.

### 3. ANALYSIS OF FLOW FIELD THROUGH WICKET GATE

#### 3.1 Preliminary Assumptions and Governing Equations

Experimental studies have shown that, for a given draft tube shape, the frequency and pressure parameters are independent of Reynolds number for Reynolds numbers greater than  $1 \times 10^5$  [2,5,6]. This is an important consideration, since turbine prototype Reynolds numbers exceed  $1 \times 10^5$ , and, thus, studies of surge can be conducted eliminating Re as a variable. It has also been found experimentally [2,5,6] that, for a particular draft tube, the frequency and pressure parameters correlate with the momentum parameter, and a critical value of the momentum parameter ( $\Omega D / \rho Q^2$ ) exists above which surge will occur. These facts have enabled extensive studies to be conducted on models of various types of draft tubes and for different values of (L/D), from which the pressure and frequency parameters can be correlated with the momentum parameter and used to predict surge for prototype installations [4].

The correlation of draft tube surge characteristics with the momentum parameter brings the realization of the importance of accurately calculating this parameter. The most convenient way to evaluate the momentum parameter is to determine the angular momentum of the flow leaving the wicket gates and subtract from this value the angular momentum removed by the turbine

runner. The momentum parameter for the flow in the draft tube can thus be written as:

$$\frac{\Omega D}{\rho Q^2} = \left[ \frac{\Omega D}{\rho Q^2} \right]_i - \frac{PD}{\rho \omega Q^2} \tag{14}$$

where

P = turbine power output

$\omega$  = angular velocity of the turbine.

The second term on the right of Equation (14) represents the change in angular momentum across the turbine runner and is evaluated from the turbine performance characteristics usually obtained from model studies. The first term on the right is the momentum parameter for the flow leaving the wicket gates and is currently evaluated using the graphical approach of [5] and illustrated by Figure 10. With this approach, the flow is assumed to leave the wicket gates perpendicular to the minimum cross section between the trailing edge of one wicket gate and the adjacent wicket gate. Referring to the nomenclature defined in Figure 10, the momentum parameter at the exit of the wicket gates can be computed by the following expression:

$$\left[ \frac{\Omega D}{\rho Q^2} \right]_i = \frac{D r_1 \sin \alpha}{BNs} \tag{15}$$

where

B = depth of the wicket gates

N = number of wicket gates.

Although the most convenient way of calculating the momentum parameter is to use the approach expressed by Equation (14), it is mentioned in References [3] and [4] that the graphical method of evaluating the first term of Equation (14) may be seriously affecting the accuracy of using the momentum parameter to correlate experimental data and to predict the occurrence and characteristics of draft tube surge. For this reason, it is felt that more attention must be given to the details of the flow through the wicket gates. It is also realized that the upstream stay vanes or the inlet spiral may influence the flow leaving the wicket gates; however, these factors obviously cannot be accounted for until an analysis is employed which considers the details of the actual flow process, which is beyond the capability of the graphical approach.

With the above considerations in mind, the following presents a method to obtain a potential solution of the flow through the wicket gates and presents the results of an experimental study conducted to evaluate the accuracy of this approach. A potential flow solution was developed, because it represents the first step usually taken in a problem of this nature, which can be used as a basis for a more exact model, if necessary. Since the flow through the wicket gates is an accelerating flow, the potential flow solution is expected to yield quite satisfactory results by itself.

Several methods for analyzing the potential flow through two-dimensional rectangular cascades are presently available. One of the most general of these, capable of handling

airfoils of any arbitrary shape, is a method developed at Douglas Aircraft Corporation and referred to as the Douglas-Neumann Cascade program. A conformal transformation of a radial flow cascade to a rectangular cascade enables the use of the Douglas-Neumann Cascade program to analyze the flow in the transformed plane.

The first assumption which is necessary to analyze the flow through the wicket gates is that the flow is two-dimensional. For most turbine installations this is a very reasonable assumption, since the wicket gates themselves are two-dimensional, and the flow at the inlet and exit to the wicket gates should be predominately two-dimensional. A schematic of a turbine cross section is presented in Figure 11, showing the inlet spiral, stay vanes, wicket gates, turbine runner and draft tube. This figure is provided to illustrate that the flow passage in the region of the wicket gates is usually a straight section, which is the justification for assuming the flow is two-dimensional. With the two-dimensional flow assumption, the geometry of a segment of the wicket gate system to be analyzed is presented in Figure 12. This figure also indicates the coordinate system which is used.

The other necessary assumptions are those which are required to enable the flow to be considered a potential flow. It is, therefore, assumed there are no body forces and that the flow is steady, incompressible, inviscid and irrotational. The inviscid flow assumption is the only assumption requiring some justification. Because the flow is accelerating through the wicket gates, the effects of the boundary layers will be minimal, and

thus, an inviscid solution is actually quite realistic in this situation.

With the above assumptions, the governing equations for the flow are the equation for zero vorticity and the continuity equation. These equations expressed in polar coordinates and in terms of dimensionless variables are as follows:

$$\text{zero vorticity: } \frac{\partial v_{\theta}}{\partial R} + \frac{v_{\theta}}{R} - \frac{1}{R} \frac{\partial v_R}{\partial \theta} = 0 \quad (16)$$

$$\text{continuity: } \frac{\partial v_R}{\partial R} + \frac{v_R}{R} + \frac{1}{R} \frac{\partial v_{\theta}}{\partial \theta} = 0 \quad (17)$$

A stream function ( $\psi$ ) is defined, such that by its definition it satisfies the continuity equation.

$$v_R = \frac{1}{R} \frac{\partial \psi}{\partial \theta} \quad (18)$$

$$v_{\theta} = - \frac{\partial \psi}{\partial R} \quad (19)$$

Substituting Equations (18) and (19) into Equation (16) yields the familiar Laplace equation in polar coordinates.

$$\frac{\partial^2 \psi}{\partial R^2} + \frac{1}{R} \frac{\partial \psi}{\partial R} + \frac{1}{R^2} \frac{\partial^2 \psi}{\partial \theta^2} = 0 \quad (20)$$

Equation (20) is solved indirectly through a transformation to obtain the flow field solution through the wicket gates. The boundary conditions which must be satisfied in conjunction with Equation (20) are:

1. A specified flow direction at infinity or far upstream.
2. The wicket gates must constitute a streamline, or in other words, the velocity normal to the wicket gate surface must be zero.
3. The Kutta condition must be satisfied at the trailing edge of the wicket gates.

### 3.2 Transformation of the Flow Field

A conformal transformation was used to transform the wicket gate system into a two-dimensional linear cascade, so that the flow in the transformed plane could be analyzed using available procedures. Since the flow in the original plane is considered a potential flow and the transformation is conformal, the flow in the transformed plane is also a potential flow and can be analyzed accordingly. The transformation used is as follows:

$$Y = \theta \tag{21}$$

$$X = \ln R \tag{22}$$

By applying the chain rule and Equations (21) and (22), it is found that Equation (20) is transformed into Laplace's equation in cartesian coordinates, Equation (23).

$$\frac{\partial^2 \psi}{\partial X^2} + \frac{\partial^2 \psi}{\partial Y^2} = 0 \tag{23}$$

where

$$\text{velocity component in the X direction} = v_x = \frac{\partial \psi}{\partial Y} \quad (24)$$

$$\text{velocity component in the Y direction} = v_y = -\frac{\partial \psi}{\partial X} \quad (25)$$

The transformation of Equation (20) into Equation (23) was carried out to illustrate that, with the transformation employed, the flow in the transformed plane is indeed a potential flow and, thus, obeys the same fundamental laws as the flow in the original plane. In the actual flow analysis, the wicket gates were transformed, and the linear cascade of airfoils obtained were analyzed as if this plane was the real plane. The transformation is illustrated by Figure 13, where the wicket gate geometry previously shown in Figure 12 is shown in the transformed plane. The circular arcs labeled 1, 2, 3 and 4 in Figure 12 become vertical lines of constant X value in Figure 13 and are similarly labeled for a comparison of the two planes. It is interesting to note that the arc of  $R=1$  becomes the Y-axis of the cartesian coordinate system in the transformed plane, while the point at  $R=0$  corresponds to  $X=-\infty$  in the new plane. Similarly, radial lines of the original plane become lines of constant Y value in the transformed plane. The X-axis corresponds to the radial line at  $\theta=0$ .

The boundary conditions in the transformed plane are identical to those in the real plane. Since flow angles are not changed by a conformal transformation, the specified inlet flow angle

is the same in both planes. In addition, the velocity component normal to the surface of the transformed airfoil must be zero, and the Kutta condition must be satisfied, as in the original plane.

Relationships between the velocity components in the two planes can be found by applying the chain rule and Equations (21) and (22) to the derivatives of  $\psi$  with respect to  $\theta$  and  $R$ . It is first found that:

$$\frac{\partial \psi}{\partial \theta} = \frac{\partial \psi}{\partial Y} \quad (26)$$

and

$$\frac{\partial \psi}{\partial R} = \frac{1}{R} \frac{\partial \psi}{\partial X} \quad (27)$$

From Equations (26) and (27) and the definitions of the stream function, the desired relations between the velocities in the two planes are obtained:

$$v_R = \frac{1}{R} v_X \quad (28)$$

$$v_\theta = \frac{1}{R} v_Y \quad (29)$$

The relationship between the magnitudes of the total velocity vectors can then be expressed as:

$$V_{\text{original plane}} = \sqrt{V_R^2 + V_\theta^2} = \frac{1}{R} \sqrt{V_X^2 + V_Y^2} \tag{30}$$
$$= \frac{1}{R} V_{\text{transformed plane}}$$

### 3.3 Method of Solution in the Transformed Plane

The Douglas Neumann cascade solution [7] was used for analyzing the flow through the transformed cascade because this method of solution is capable of handling infinite cascades of airfoils of an arbitrary shape. A solution is obtained by applying a distribution of sources on the surface of the airfoils in the cascade, such that the combination of the onset velocity, the source at the particular point, and the induced velocity from the remaining source distribution satisfy the boundary condition of zero normal velocity at the surface. In a similar manner, the vorticity distribution on the airfoils is obtained by employing the same set of equations with the velocity vector of the sources rotated 90°.

The source distribution is determined by representing the airfoils as a series of straight line segments, with the source strength assumed constant over each segment and the boundary condition

satisfied at the segment midpoint. With this approximation, the induced velocity at the midpoint of a particular segment can be represented by a summation of a set of integrals representing the induced velocity from the remaining segments. Since the source strength is assumed constant over the segment, the integrals can be evaluated analytically, which results in a set of algebraic equations which must be solved simultaneously for the source strength of each segment. This technique will approach an exact solution as the number of segments approaches infinity, but sufficient accuracy is achieved as long as the straight line segments are small enough to adequately describe the airfoil shape.

The solution to the general problem is obtained by calculating the potential flow for three basic flows consisting of the solution for a flow with zero angle of attack,  $90^\circ$  angle of attack, and a pure circulatory flow. These three solutions, which all satisfy the boundary condition of a zero velocity component normal to the surface, are then combined in such a manner to satisfy the specified inlet angle and the Kutta condition. The complete solution enables the velocity components and the static pressure to be determined at any point in the flow field and also yields the overall angle by which the cascade turns the flow.

#### 3.4 Discussion of Normalizing Parameters and the Reverse Transformation

Thus far, the equations governing the flow in both planes have been presented, and the method of obtaining a solution in the transformed plane has been discussed. The equations relating the velocity

components in the two planes have also been given, however, before these equations can be specifically applied, consistent normalizing velocities must be selected in each plane. Since it is known from the conservation of mass equation that the average x component of velocity is constant both upstream and downstream of a rectangular cascade,  $\bar{v}_x$  represents a convenient parameter to normalize the velocity in the transformed plane. Although the Douglas-Neumann cascade solution uses as a normalizing parameter the modulus of the average velocity vector upstream and downstream of the cascade, the output can easily be converted so that the velocity is normalized by  $\bar{v}_x$ .

In the original plane the velocity component corresponding to  $\bar{v}_x$  is the radial component. The average radial velocity component is not constant, but, once again from the conservation of mass equation, it is known that  $r \bar{v}_r = \text{constant}$ . Using this relationship, if a reference value of  $r$  is selected, a corresponding reference value of  $\bar{v}_r$  can be obtained. The value of  $r$  which is convenient for this purpose is the radius of the wicket gate spindle centers ( $r_s$ ). Selecting  $r_s$  as the reference radius results in the following definition of the normalizing velocity in the original plane.

$$v_{r_s} = Q / (2\pi B r_s) \quad (31)$$

It is apparent from the definition that  $v_{r_s}$  represents the average radial velocity which would exist at the spindle radius if the wicket gates were not present.

Rewriting Equation (28) in terms of dimensional quantities allows the relationship between the velocities in the planes to be determined when they are normalized using the above parameters. For

the present,  $v_x$  will be normalized by the temporary variable,  $v_{ref}$

$$\frac{v_r}{v_{r_s}} = \frac{c}{r} \frac{v_x}{v_{ref}} \quad (32)$$

To relate the two normalizing velocities, it is known that  $v_x$  should equal  $\bar{v}_x$  when  $v_r = v_{r_s}$  and  $r=r_s$ . Solving Equation (32) for  $v_{ref}$  after inserting these values yields

$$v_{ref} = \bar{v}_x \frac{c}{r_s} \quad (33)$$

Substituting Equation (33) back into Equation (32) provides the new relationship for relating the dimensionless radial velocity in the original plane to the x component of velocity in the transformed plane.

$$v_r = \frac{v_r}{v_{r_s}} = \frac{c}{r} \frac{v_x}{\bar{v}_x \frac{c}{r_s}} = \frac{r_s}{r} \frac{v_x}{\bar{v}_x} = \frac{R_s}{R} \frac{v_x}{\bar{v}_x} \quad (34)$$

Similarly,

$$v_\theta = \frac{v_\theta}{v_{r_s}} = \frac{R_s}{R} \frac{v_y}{\bar{v}_x} \quad (35)$$

and

$$v = \frac{v_{\text{original plane}}}{v_{r_s}} = \frac{R_s}{R} \frac{v_{\text{transformed plane}}}{\bar{v}_x} \quad (36)$$

These equations provide the necessary relationships for the reverse transformation of the solution from the transformed plane to the original plane. It should be noted that the fluid angles are not changed by the transformation, thus, the above equations need only to be applied when interested in the velocity magnitudes. Equation

(36) is used in the computer program to transform the local velocity on the surface of the blades, thus, enabling the pressure distribution on the wicket gate to be determine.

### 3.5 Analytical Study Conducted

The method of transforming the wicket gates and employing the rectangular cascade analysis to obtain a potential flow solution was used to analyze the flow through the wicket gates of an air model. This model, which was primarily fabricated to conduct draft tube surge studies, will be described in the next section on the experimental study. The wicket gates shown in Figure 12 are a scale drawing of the real wicket gates in the model. These wicket gates have no camber, a chord length of 3.97 cm (1.562 in.), and a maximum thickness of 0.544 cm (0.214 in.).

Solutions were obtained for the wicket gates with angular settings between 0 and 80° in 10° increments. These angles are measured between the wicket gate chord and a radial line. The closed position is at the angular setting of 83°. Two solutions were obtained for each wicket gate setting, one with the flow entering radially and the other solution with the flow at a zero angle of attack in the transformed plane. These two solutions were obtained to evaluate the influence of the upstream flow on the fluid exit angle. It was found that for the present wicket gate geometry the inlet angle did not affect the exit angle. This conclusion cannot be made for all systems, however, since even for a potential flow solution the spacing between gates will affect the amount of turning the cascade can perform. The

present method of solution could be used by testing various spacings to determine what spacing is needed to eliminate upstream effects.

The graphical method indicated by Figure 10 was also carried out, and these results will be presented along with the experimental results and potential flow solution. Initial results comparing the fluid exit angles predicted by the graphical approach and the potential flow solution revealed very little difference. The question was then raised, would cambered wicket gates demonstrate a larger deviation between the fluid angles predicted using the two methods? To study this possibility, an analytical study was conducted for cambered wicket gates similar to the study for the symmetrical wicket gates. For this case, the results from the potential solution also revealed no significant dependence on the inlet angle. However, a slightly larger deviation was found between the fluid exit angle predicted by the potential solution and the graphical approach. The actual numerical results will be presented in a following section on analytical and experimental results.

### 3.6 Experimental Program

A sketch of the test facility used to obtain experimental data for comparison with the potential flow solution is shown in Figure 14. In this facility, flow surveys were made at a constant radius behind several wicket gate channels, with measurements made every 1.5 degrees. In addition to the open inlet configuration shown in the figure, tests were also conducted with an inlet spiral installed. The tests with and without the inlet spiral enabled the effects of the inlet flow angle on the exit flow from the wicket gates to be investigated. The draft

tube has an inlet diameter of 15.56 cm (6.125 in.) and the probe was located at a diameter of 22.86 cm (9.0 in.).

Total pressure, static pressure and the flow angles were measured using a three-hole prism type probe. The flow angle was determined by nulling the probe. The total pressure was measured from the center hole, and the static pressure was calculated from the average pressure of the two side holes and a pressure coefficient obtained during a static pressure calibration of the probe. All pressures were measured with a variable-reluctance differential pressure transducer with the voltage output measured by an integrating digital voltmeter.

The velocity magnitude and flow angles, which varied across a wicket gate channel, were used to calculate the momentum parameter by numerically integrating the flow characteristics across a channel to obtain the flow rate and the angular momentum flux. This momentum parameter was then used to calculate an average flow angle for comparison with the theoretical predictions. For a flow with uniform velocity, it can be shown that the only flow characteristic influencing the momentum parameter is the flow angle, as expressed by the following relation:

$$\frac{\Omega D}{\rho Q^2} = \frac{D}{2\pi B} \tan \bar{\alpha} \quad (37)$$

where

$\bar{\alpha}$  = the flow angle for a uniform flow, or the average flow angle for a nonuniform flow yielding the equivalent moment parameter.

40

Equation (37) was used for calculating  $\bar{\alpha}$  from the momentum parameter obtained experimentally. An average flow angle was also calculated by simply computing the arithmetic average of all the measured local flow angles. These two average angles were almost identical, however, and future references to the average angle will not mention the method of calculation.

### 3.7 Discussion of Analytical and Experimental Results

The downstream flow angle obtained from the potential flow solution in the transformed plane is the angle of the uniform flow theoretically achieved at negative infinity. For all practical purposes, however, uniform flow of constant angularity is achieved a short distance from the trailing edge of the blades. When applying the potential flow solution to a real situation, the flow may or may not become uniform before it reaches the location of the turbine runner. It should be pointed out that even if sufficient spacing for the flow to become uniform is not available, the uniform flow angle still applies for calculating the momentum parameter, since no change in the momentum parameter will occur between the trailing edge and the location where uniform flow would be achieved. With this in mind, the flow angle calculated by the potential theory for the symmetrical wicket gate is presented in Figure 15 as a function of wicket gate angle. The angles from the potential theory are represented by the solid line.

The average fluid angles obtained experimentally are also presented in Figure 15. No difference was found in the measured angles for the two sets of tests conducted both with and without the inlet spiral, thus, only one set of data is presented. The fact that the exit flow angles did not change with the different

inlet configurations is consistent with the predicted data which also showed no effect with the change in the angle of attack.

The graphical method for predicting the momentum parameter, indicated by Figure 10, was used to calculate the exit flow angle from the wicket gates to provide an additional comparison and demonstrate if any improvement is achieved by the potential flow solution. The flow angle ( $\alpha$ ) defined in Figure 10 is not the average flow angle, however, since the angle is defined within the wicket gate passage and does not represent the angle obtained when the flow becomes uniform. The angle ( $\alpha$ ) can be used with Equation (15) to calculate the momentum parameter, and then with the momentum parameter the average flow angle ( $\bar{\alpha}$ ) can be calculated from Equation (37). The average flow angles calculated in this manner are the data represented by the circles in Figure 15.

For the system with the symmetrical wicket gates, as shown by Figure 15, the results from both the potential flow solution and graphical method agree very closely with the experimental data. At the higher wicket gate angles the potential solution is only approximately 1 degree low in its prediction of the fluid angle. At the lower wicket gate settings the potential solution predicts values approximately 2 degrees higher than the measured angles. On the other hand, the graphical method shows its greatest deviation at the higher wicket gate angles, where flow angle is under-predicted by approximately 4 degrees. At the lower wicket gate angles, the fluid angles from the graphical method and the experimental data are approximately equal.

With the deviation between the predicted and experimental data of such a small magnitude, it is difficult to conclude whether the deviation is due to a minor shortcoming of the prediction methods or due to an error in the experimental data. The fact that the experimental data does not appear to be exactly approaching the origin leads one to believe the deviation may be due to experimental error. At the lower wicket gate angles, the probe traverses were nearer to the trailing edge of the wicket gates, and some measurements were, therefore, made with the probe partially in the wakes of the gates. If the measurements were not perfectly centered around the wakes, the error in the angle measurements would not be completely canceled out by the averaging process, resulting in one possible source of error. An additional source of error could be the angle of the wicket gates. The linkage, which controls the angles of the wicket gates, has some hysteresis, which may be enough to allow the gates to be at a slightly different angle than expected.

Over the full range of wicket gate angles the potential solution appears to be slightly more accurate than the graphical method for the symmetrical wicket gate geometry. However, the very small difference between the predictions by both methods and the experimental data does not give one method a significant advantage over the other. It was for this reason that an analytical study of a system with cambered wicket gates was undertaken to investigate if the two methods differ more significantly for cambered wicket gates. The geometry of the wicket gate selected for the study is

pictured in Figure 18. The results from the study are presented in Figure 16, where the fluid angles predicted by the two methods are plotted similarly to the previous data. Figure 16 shows a slightly larger difference between the two methods than was observed for the symmetrical wicket gate, although the difference is still not extremely large. For the cambered wicket gate the maximum difference is approximately 6 degrees while for the symmetrical wicket gate the difference is approximately 3.5 degrees. For the cambered wicket gates the potential flow solution is expected to yield the more accurate results, since it can account for the details of the wicket gate shape. The significance of this conclusion should be determined, however, and cambered wicket gates should be studied experimentally in the future. One advantage of the potential flow solution is that stay vanes can be added to the analysis for cases where the gate spacing is such that inlet conditions to the gates will affect the exit flow angle. The pressure distribution on the wicket gates can also be obtained from the potential flow solution, from which the force and moment coefficients for the spindle can be calculated.

Before concluding this section on the theoretical and experimental results, an additional comparison is made between the local fluid angles measured and the fluid angles predicted at the probe radius for the symmetrical wicket gate. Only the potential flow solution is capable of calculating the local flow properties, and the comparison of the flow angle distributions is made to demonstrate these capabilities. Figure 17 presents the flow angles predicted and measured downstream of several wicket gate passages. The positive direction of the circumferential location coordinate is in

the same direction as the mean swirl of the flow and opposite to the positive  $\theta$  direction shown in Figure 12. In general, Figure 17 shows that the predicted and measured data have the same trends and that the slope of data is almost identical. The mean value of the two sets of data is the main difference, which tends to make the prediction look worse than it is. The mean values differ only by approximately 2 degrees. It should be pointed out that the large extreme angles in the experimental data are erroneous measurements made with the probe in the wake of wicket gates. Eliminating these points would make the prediction appear more accurate.

### 3.8 Summary and Conclusions

A two-dimensional potential flow solution has been presented for the flow through a radial cascade, such as the wicket gates of a hydraulic turbine. Comparisons of the predicted flow angles from the potential solution and the angles measured in an air model of a wicket gate system indicate that the potential theory very adequately describes the real fluid characteristics. For the wicket gate system investigated, little difference was found between the potential flow solution and a graphical method currently used. A purely analytical study of cambered wicket gates was conducted which showed a slightly larger deviation between the two methods. It is expected that the potential solution yields the more accurate results, although this conclusion was not verified experimentally. For the present, the main advantages of the potential flow solution are the ability to obtain a more detailed solution of the flow and the ability to include upstream effects if they are considered to be influential. The pressure distribution on the wicket gates is also obtained, and the force and moment coefficients for the wicket gate spindles can be computed.

References

- [1] Falvey, H. T., "Draft Tube Surges--A Review of Present Knowledge and an Annotated Bibliography," Report No. REC-ERC-71-42, U. S. Bureau of Reclamation, Denver, Colorado, December 1971.
- [2] Cassidy, J. J., "Experimental Study and Analysis of Draft-Tube Surging," Report No. REC-OCE-69-5, U. S. Bureau of Reclamation, Denver, Colorado, October 1969.
- [3] Palde, U. J., "Model and Prototype Turbine Draft Tube Surge Analysis by the Swirl Momentum Method," IAHR and AIRH Symposium, 1974.
- [4] Palde, U. J., "Influence of Draft Tube Shape on Surging Characteristics of Reaction Turbines," Report REC-ERC-72-24, U. S. Bureau of Reclamation, Denver, Colorado, 1972.
- [5] Falvey, H. T. and Cassidy, J. J., "Frequency and Amplitude of Pressure Surges Generated by Swirling Flow," Transactions of Symposium Stockholm 1970, International Association for Hydraulic Research, Part 1, Paper E1, Stockholm, Sweden, 1970.
- [6] Cassidy, J. J. and Falvey, H. T., "Observations of Unsteady Flow Arising After Vortex Breakdown," Journal of Fluid Mechanics, Vol. 41, Part 4, pp. 727-736, 1970.
- [7] Giesing, J. P., "Extensions of the Douglas Neumann Program to Problems of Lifting, Infinite Cascades," U. S. Department of Commerce, Report No. LB 31653, AD 605207, revised July 2, 1964.

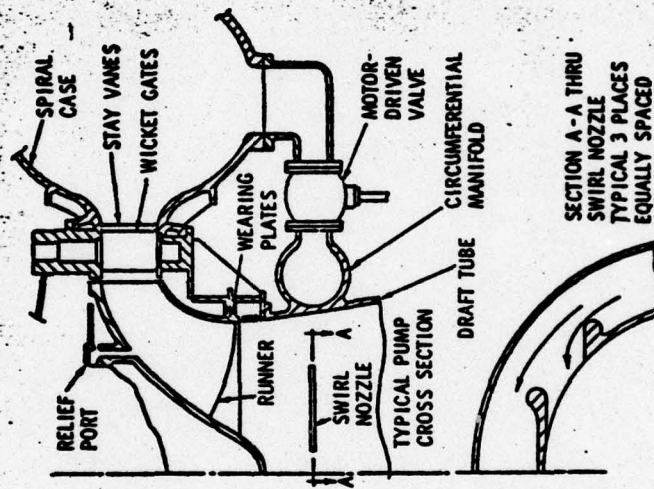


Figure 1 - Schematic of Proposed Means of Preventing Draft Tube Surge

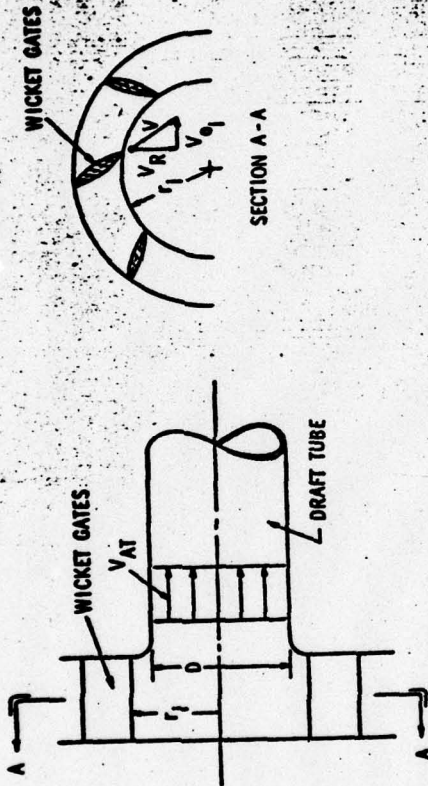


Figure 2 - Schematic of Flow Leaving Wicket Gates

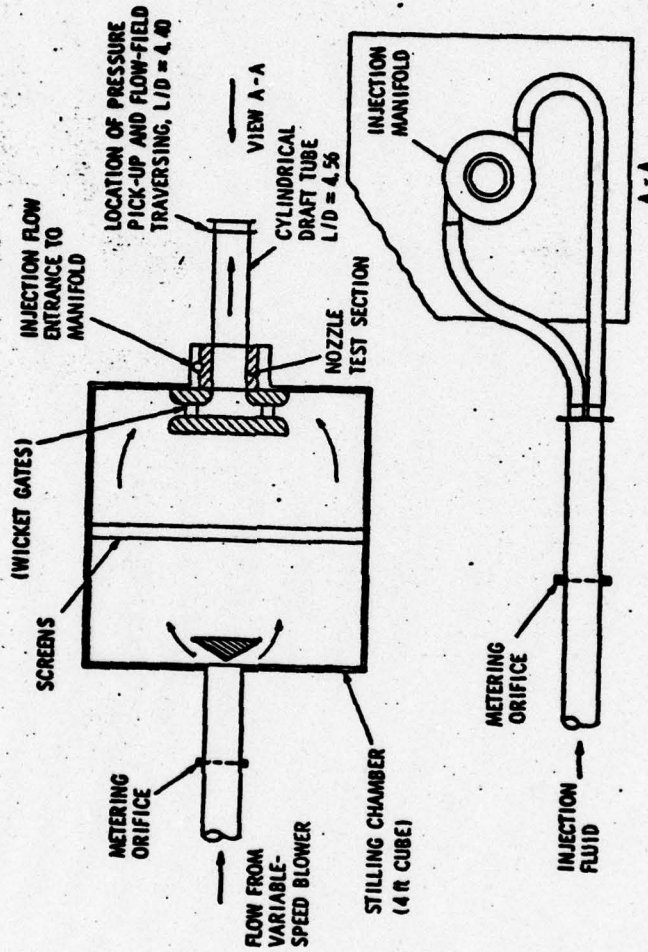


Figure 3 - Schematic of Air Flow Facility

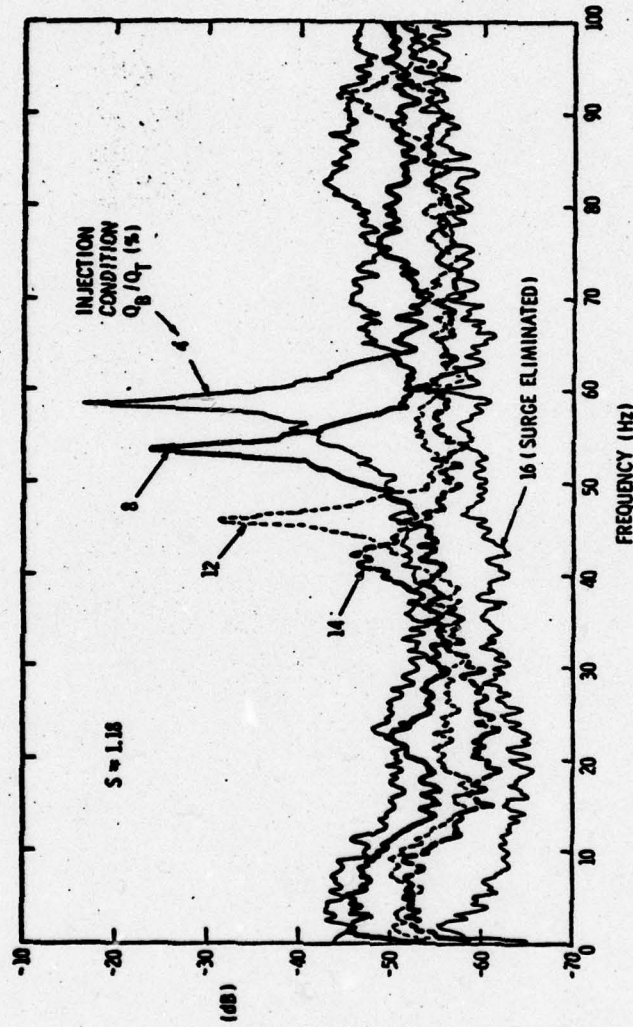


Figure 4 - Spectral Analysis of Surge

50

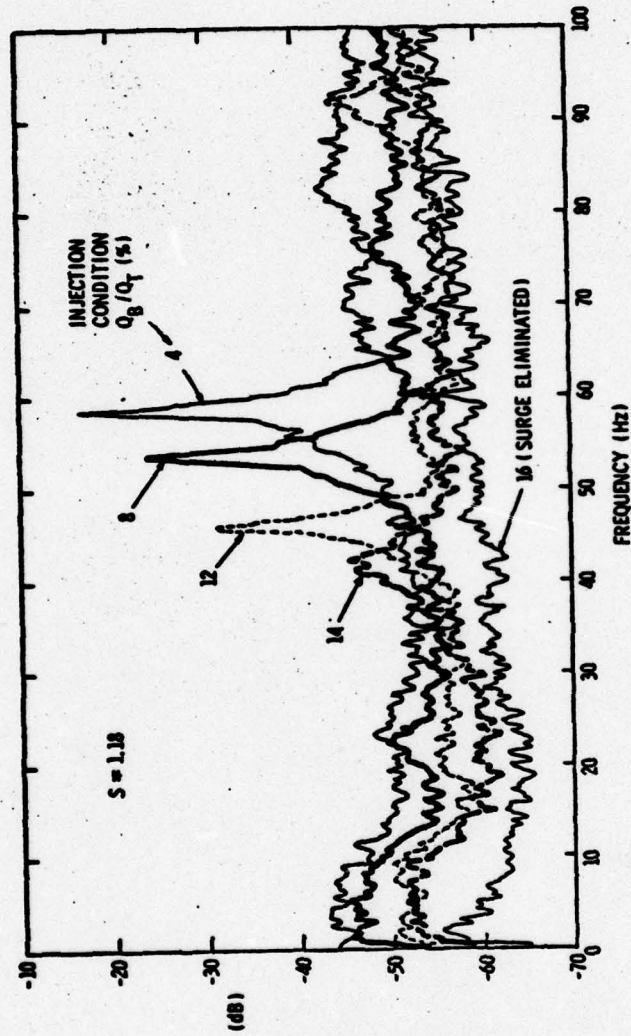


Figure 4 - Spectral Analysis of Surge

50

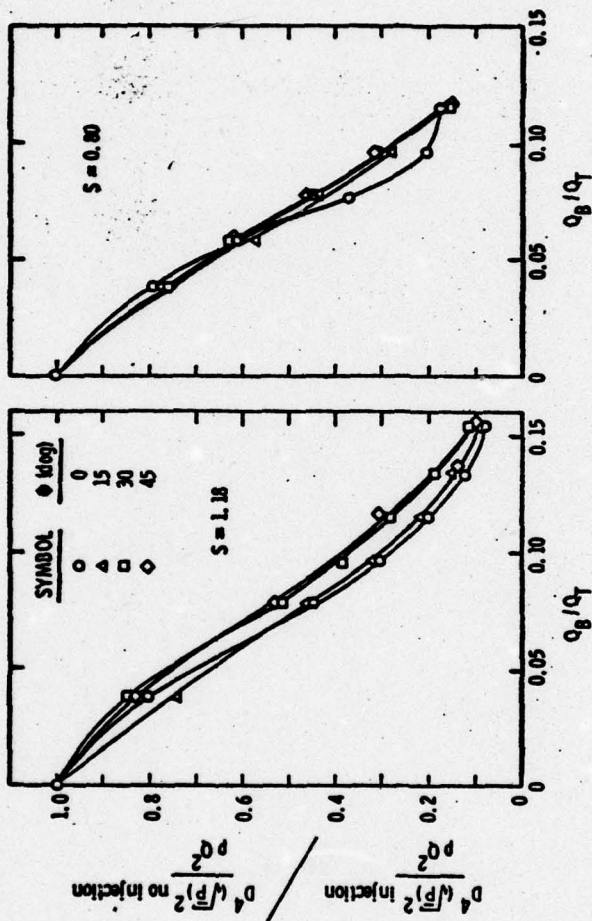


Figure 5 - Comparison of Nozzle Angle of Injection

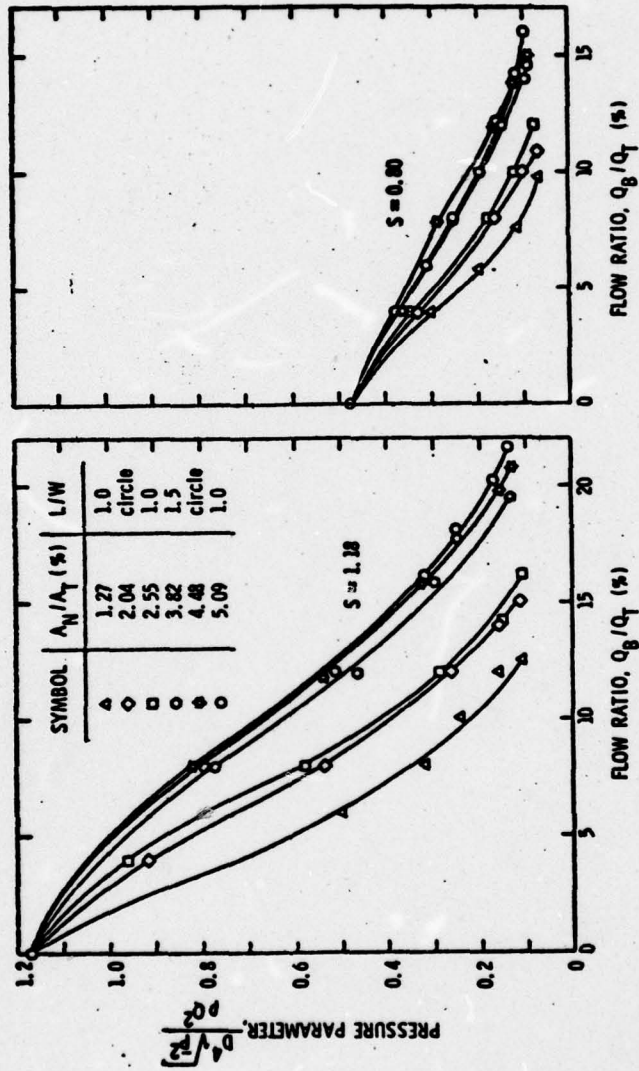


Figure 6 - Comparison of Nozzle Geometries

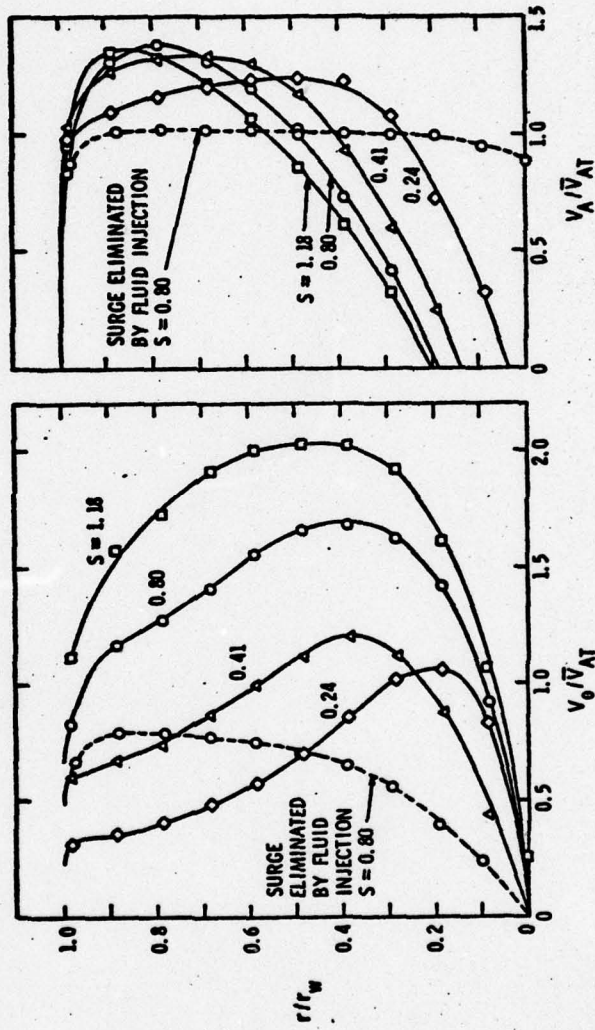


Figure 7 - Axial and Tangential Velocity Distribution

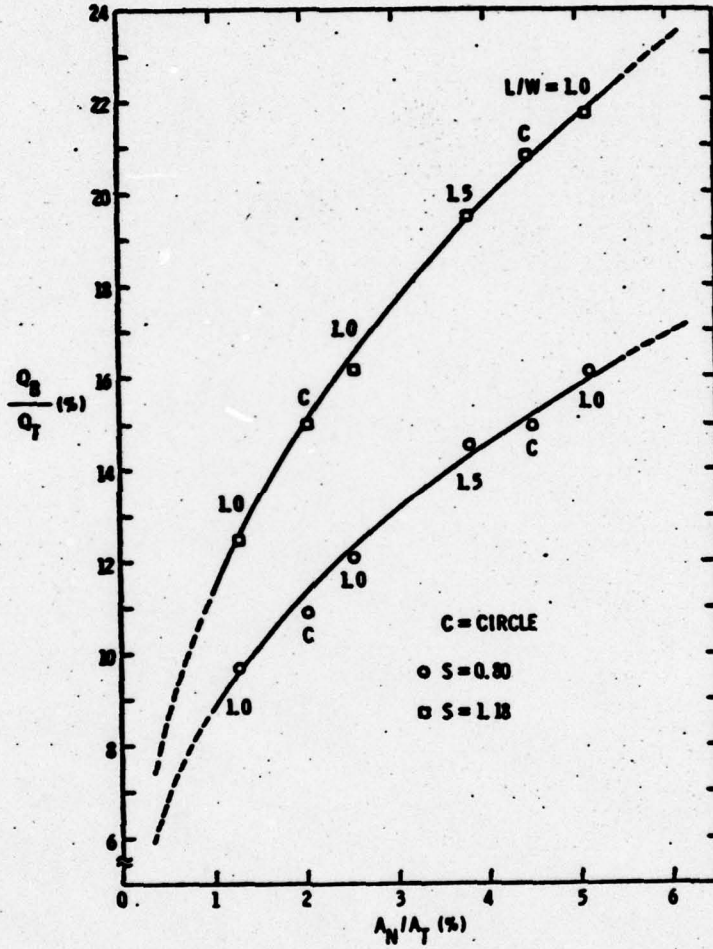


Figure 8 - Injected Flow Required to Eliminate Surge for Cylindrical Draft Tube

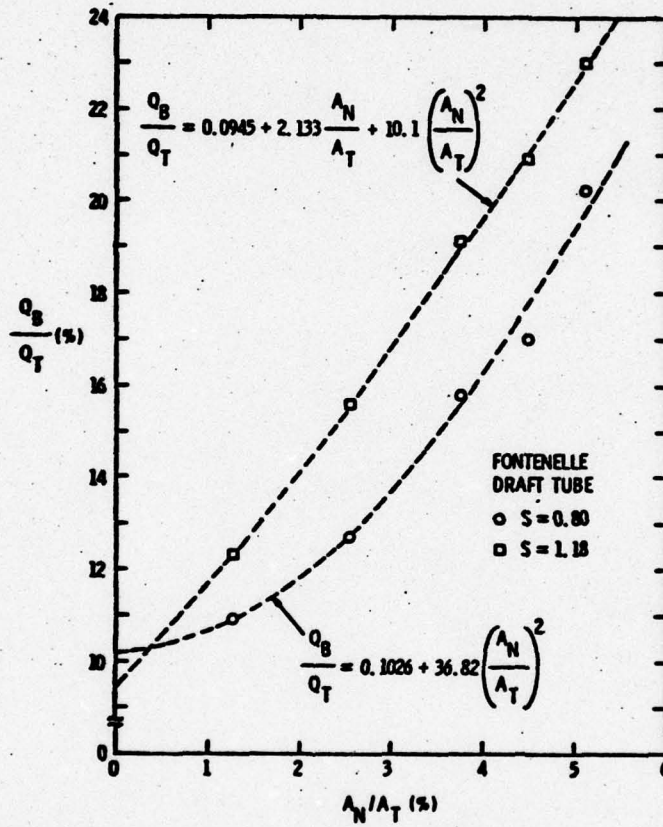


Figure 9 - Injected Flow Required to Eliminate Surge for Elbow Draft Tube

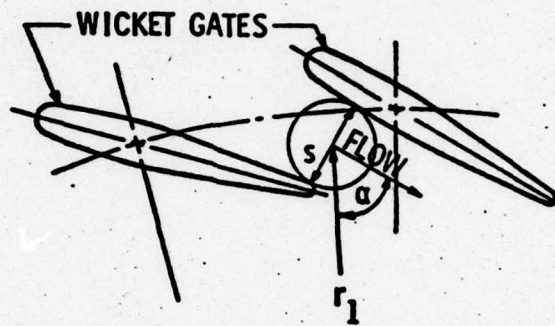


Figure 10 - Schematic of Two Wicket Gates Illustrating the Graphical Method of Determining the Flow Angle and, hence, the Momentum Parameter

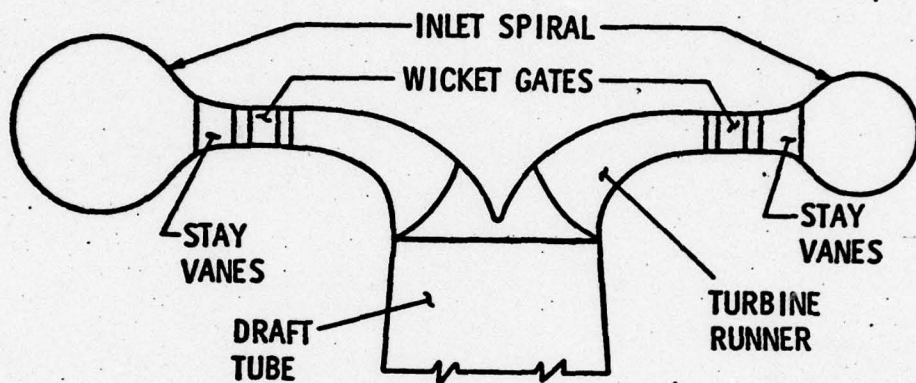


Figure 11 - Schematic of a Turbine Cross Section Illustrating the Geometry of the Flow Passage in the Region of the Wicket Gates

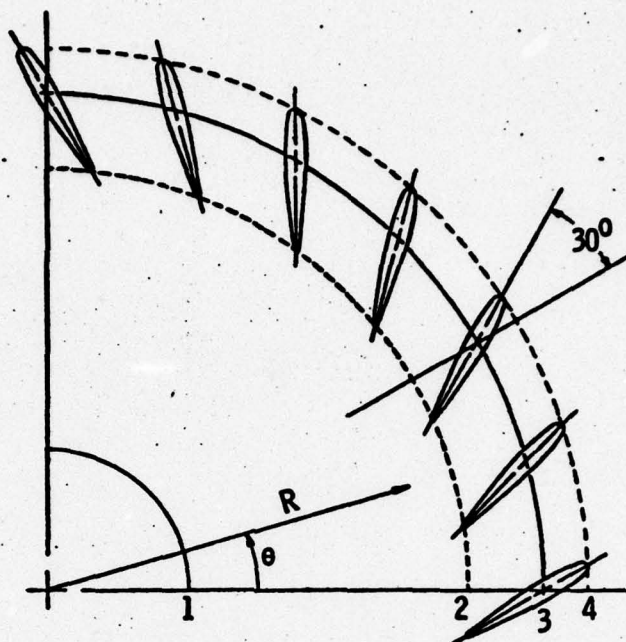


Figure 12 - Schematic of a Sector of a Wicket Gate System in the Real Coordinate System

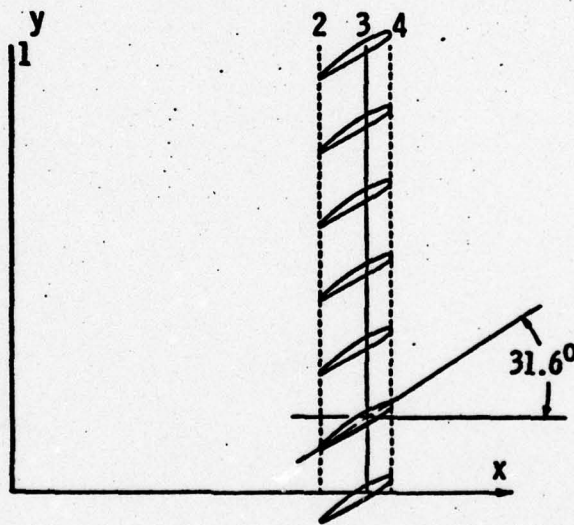


Figure 13 - Schematic of the Two-Dimensional Cascade Obtained by Transforming the Wicket Gate System

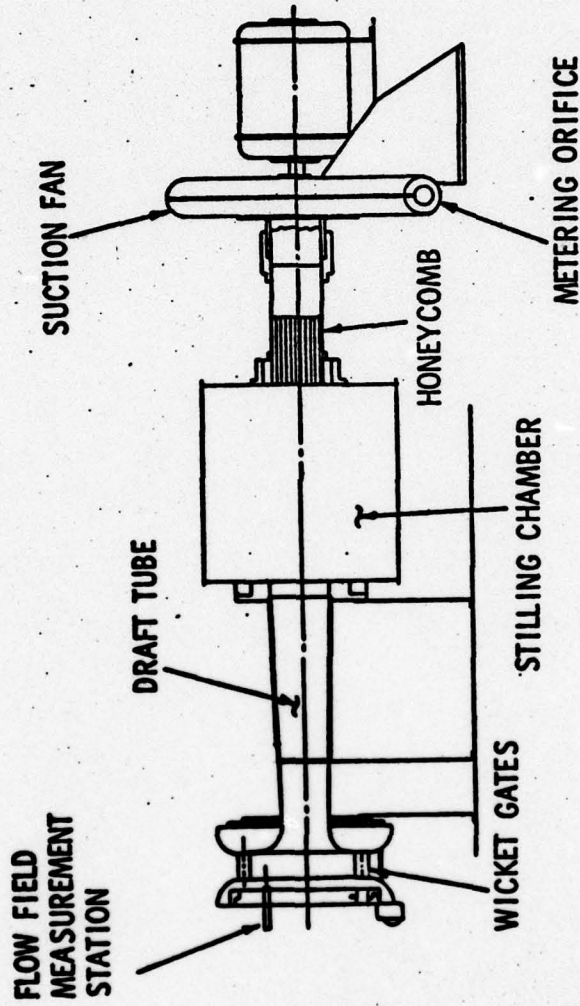


Figure 14 - Sketch of the Wicket Gate and Draft Tube Model Used to Experimentally Evaluate the Potential Flow Solution

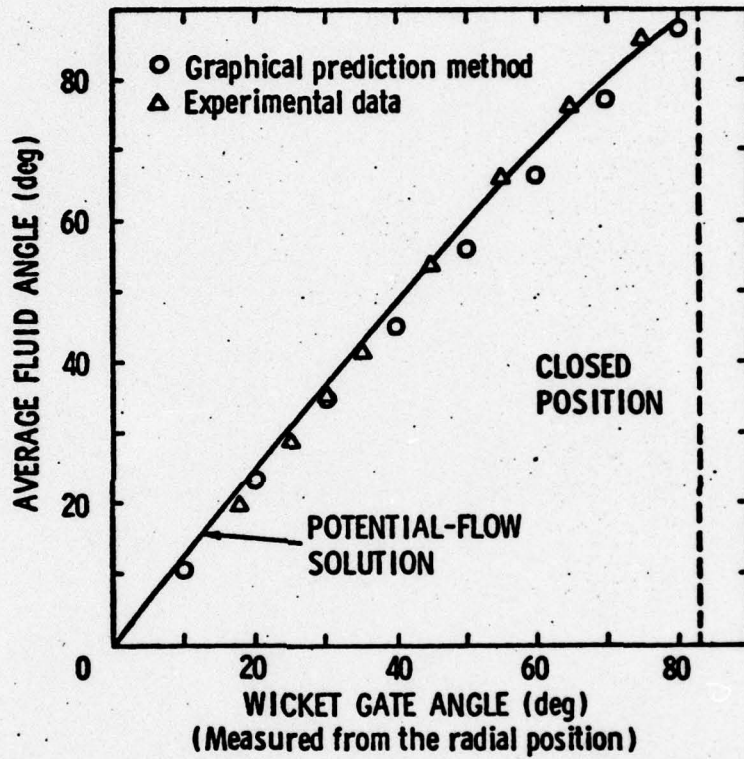


Figure 15 - Average Flow Angle versus Wicket Gate Angle Obtained for the Symmetrical Wicket Gates from the Potential Flow Solution, Graphical Prediction Method, and Experimental Data

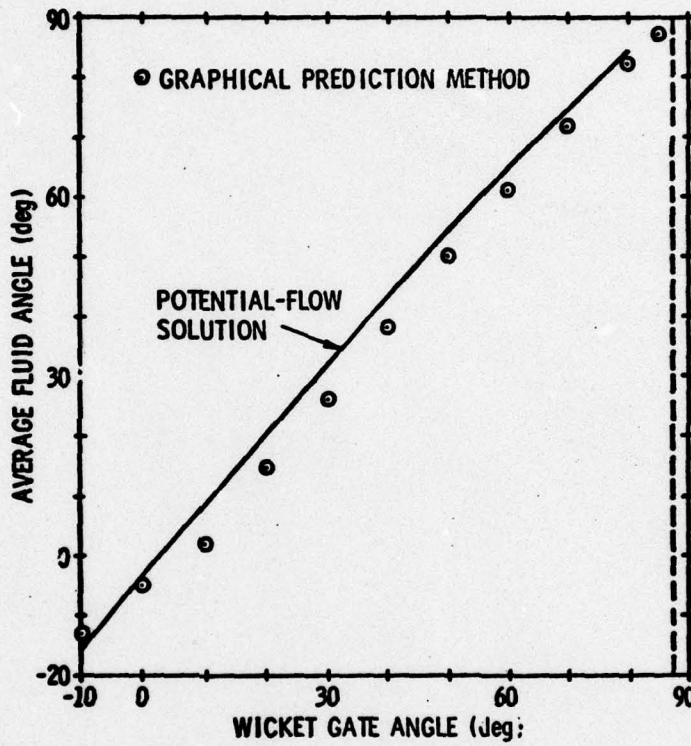


Figure 16 - Comparison of the Fluid Exit Angles Predicted for the Cambered Wicket Gate System Using the Potential Flow Solution and the Graphical Approach

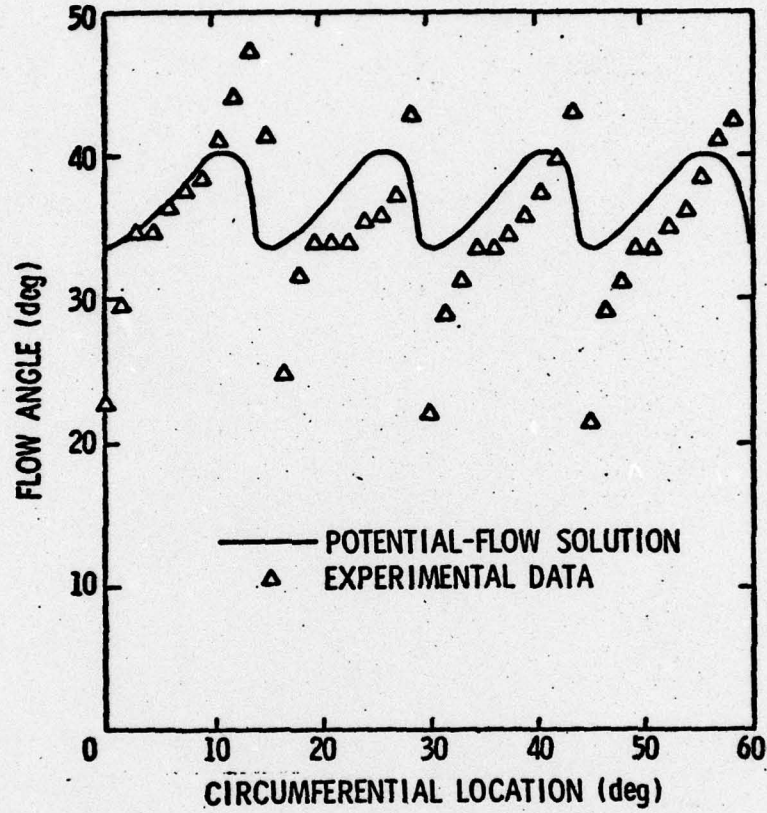


Figure 17 - Local Fluid Angle versus Circumferential Location Measured Downstream of the Wicket Gates and Predicted by the Potential Flow Solution



### Appendix A

#### Results of Preliminary Tests Indicating Effect of Test Apparatus Geometry on Surge Pressure

The test facility for the draft tube surge study as shown in Figure 3 was not the original test apparatus considered in the program. The original draft tube surge test facility was designed, fabricated, and assembled as shown in Figure 14. The main difference between the original test facility and the one finally used for testing is the location of the air supply flow fan. In the original test facility, (Figure 14), air was drawn from the open atmosphere into the test section and dumped into a stilling chamber by means of a flow fan downstream of the draft tube. In the final test facility, (Figure 3), air was blown into a stilling chamber first, then passed through the test section and dumped to atmosphere.

Examination of the sketches of the two facilities would seem to indicate that the important flow characteristics (pressure parameter and frequency parameter) produced in either test facility would be essentially the same. The authors felt that it was important for the test facility to produce relations between the surge parameters and the momentum parameter similar to those obtained by Palde [4]. Preliminary tests in the original test apparatus provided a relation between frequency parameter and momentum parameter much like that obtained by Palde. However, pressure parameter as a function of momentum parameter was essentially constant, which radically disagreed with Palde's data. In an attempt to obtain pressure parameter data similar to Palde's, various pressure pick-up devices were tried at various locations along the draft tube. After repeated failure to obtain the desired data in the original test facility, a test facility similar to that

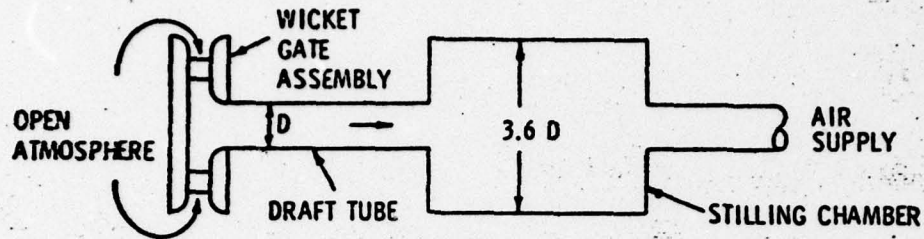
used by Palde (i.e., pushing air through the draft tube and dumping to atmosphere) was constructed as shown in Figure 3. Surging characteristics obtained in the modified test facility agreed very well with Palde's data. The altered test facility solved the problem but raised a question. Why was the pressure parameter much lower for the original test facility compared to that obtained in Palde's or the final test facility? Velocity profiles obtained in the draft tube at  $L/D=4.40$  for each facility at various momentum parameters were compared. Figure A.1 shows that the velocity profiles are quite similar for both test facilities.

In an effort to answer this question, a brief series of tests were performed to investigate the effects on pressure parameter of dumping the draft tube flow into a stilling chamber and then dumping to atmosphere. Tests were performed on both the cylindrical and elbow type draft tubes. Tables A1 and A2 show the different geometries that were investigated. With any given facility geometry tested, a survey of pressure parameter as a function of momentum parameter was obtained. The flowrate through the test facility was measured by an orifice meter and the surge pressure was measured through a dynamically calibrated pressure transducer by an RMS meter as earlier described in this report.

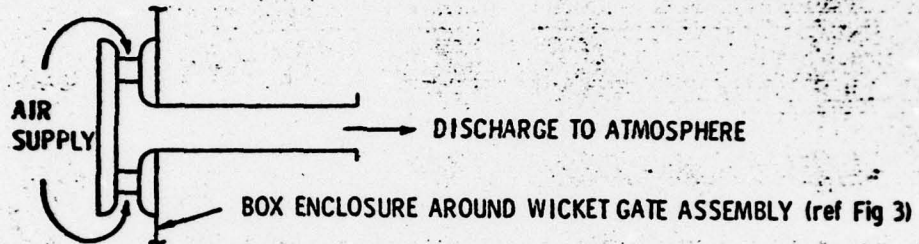
Figure A.2 shows the results of this investigation for the cylindrical draft tube and likewise, Figure A.3 corresponds to the Fontenelle (elbow type) draft tube. The numbers on the curves in Figures A.2 and A.3 correspond to the geometries so numbered in Tables A1 and A2. Comparison of curves (1) and (2) in Figure A.2 shows the effects of a stilling chamber below the draft tube on pressure parameter. Looking at all the curves of both Figures A.2 and A.3, it is obvious that the use of the stilling chamber in all cases reduced the pressure parameter

Table A.1

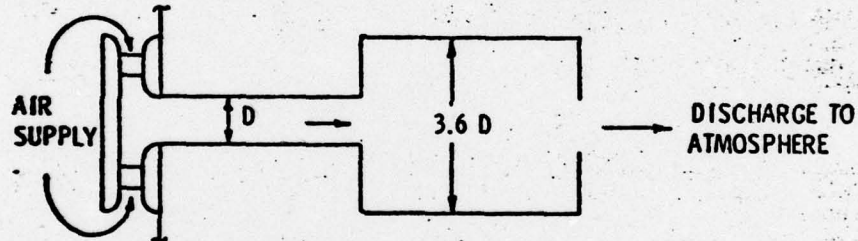
1. STILLING CHAMBER AND AIR SUPPLY DOWNSTREAM OF DRAFT TUBE



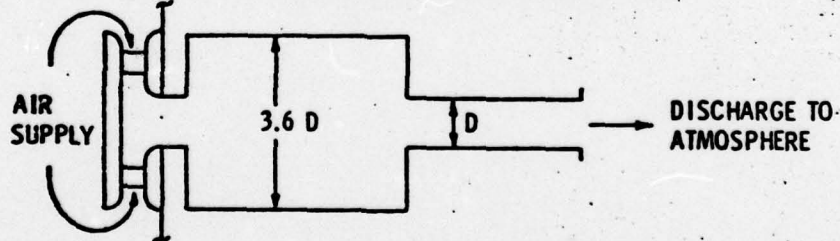
2. NO STILLING CHAMBER, UPSTREAM AIR SUPPLY



3. STILLING CHAMBER DOWNSTREAM OF DRAFT TUBE, UPSTREAM AIR SUPPLY



4. STILLING CHAMBER AND AIR SUPPLY UPSTREAM OF DRAFT TUBE



5. STILLING CHAMBER WITH SCREEN DOWNSTREAM OF DRAFT TUBE, UPSTREAM AIR SUPPLY

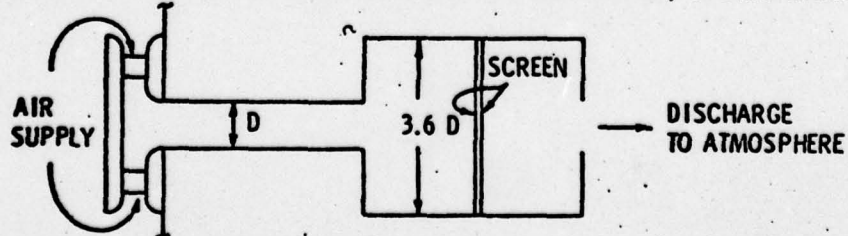
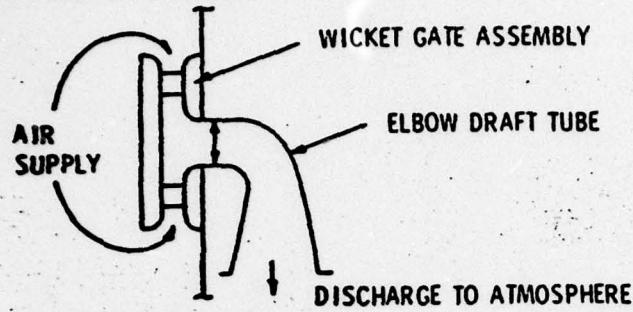
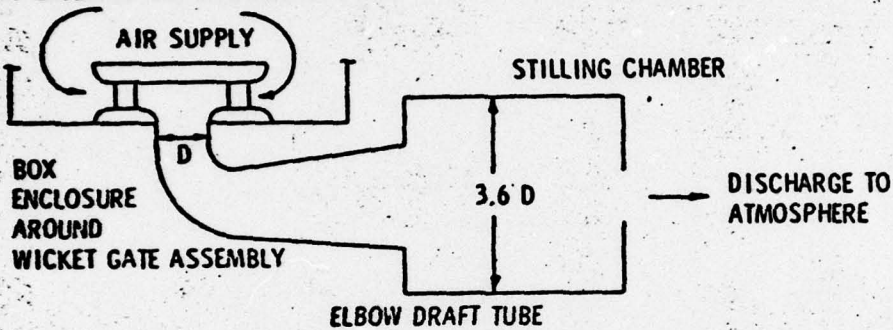


Table A.2

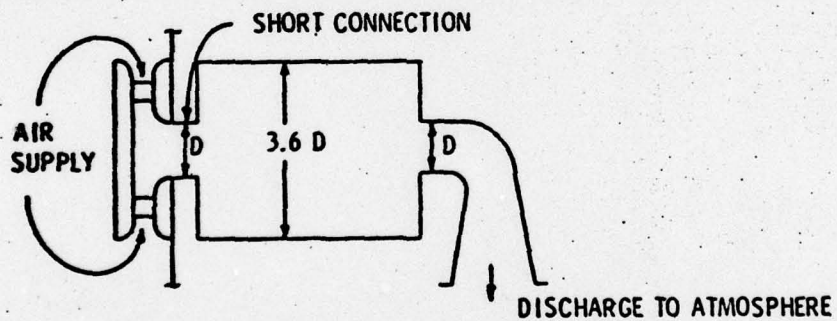
1. NO STILLING CHAMBER, UPSTREAM AIR SUPPLY



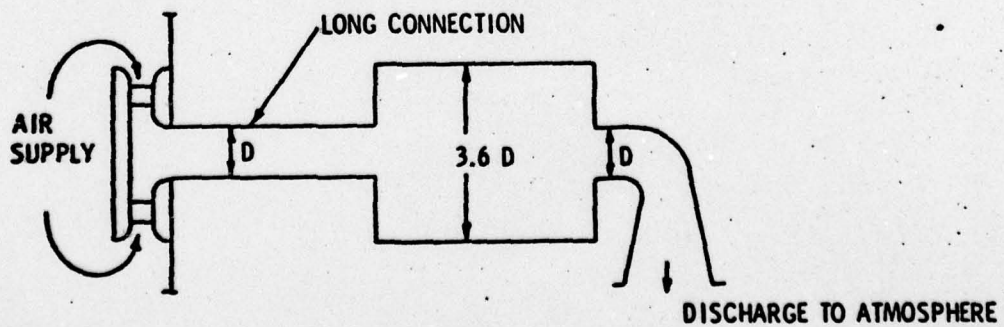
2. STILLING CHAMBER DOWNSTREAM OF DRAFT TUBE, UPSTREAM AIR SUPPLY



3. STILLING CHAMBER (SHORT CONNECTION) UPSTREAM OF DRAFT TUBE, UPSTREAM AIR SUPPLY



4. STILLING CHAMBER (LONG CONNECTION) UPSTREAM OF DRAFT TUBE, UPSTREAM AIR SUPPLY



magnitude. Notice that screens placed across the stilling chamber (curve (5), Figure A.2) forced the pressure parameter relation of the original test facility to become almost identical to those of Palde and curve (2).

Out of this brief study comes speculation that stilling chambers placed downstream of a turbine runner may be an effective means of reducing draft tube surge in hydroelectric pump-turbines. Further study is required in this area.

A second complication has been suggested by H. Falvey of The Bureau of Reclamation. This involves the geometry of model test loops which have stilling chambers located up or downstream of model pump-turbines. The water level and geometry of these chambers could provide surge characteristics, based on model tests, that are inconsistent with those of the prototype.

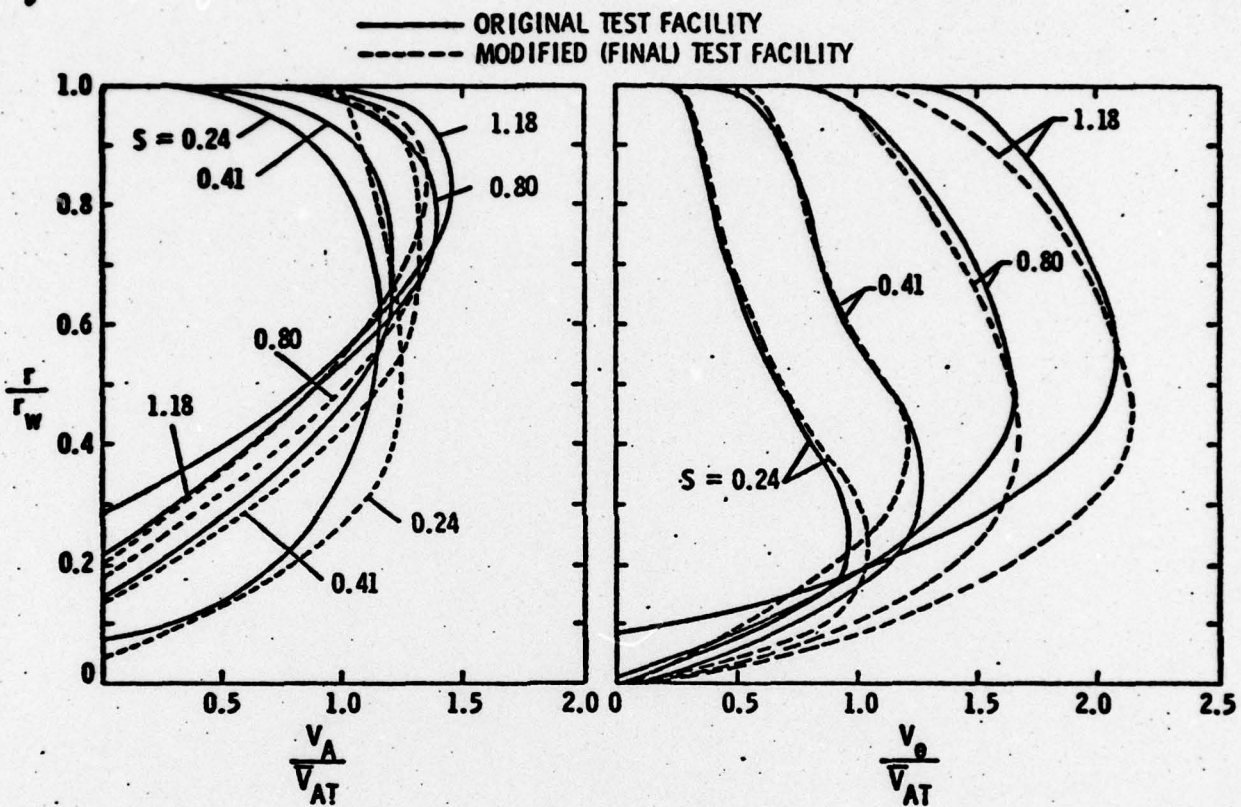


Figure A.1 - Axial and Tangential Velocities in the Original and Modified Test Facility

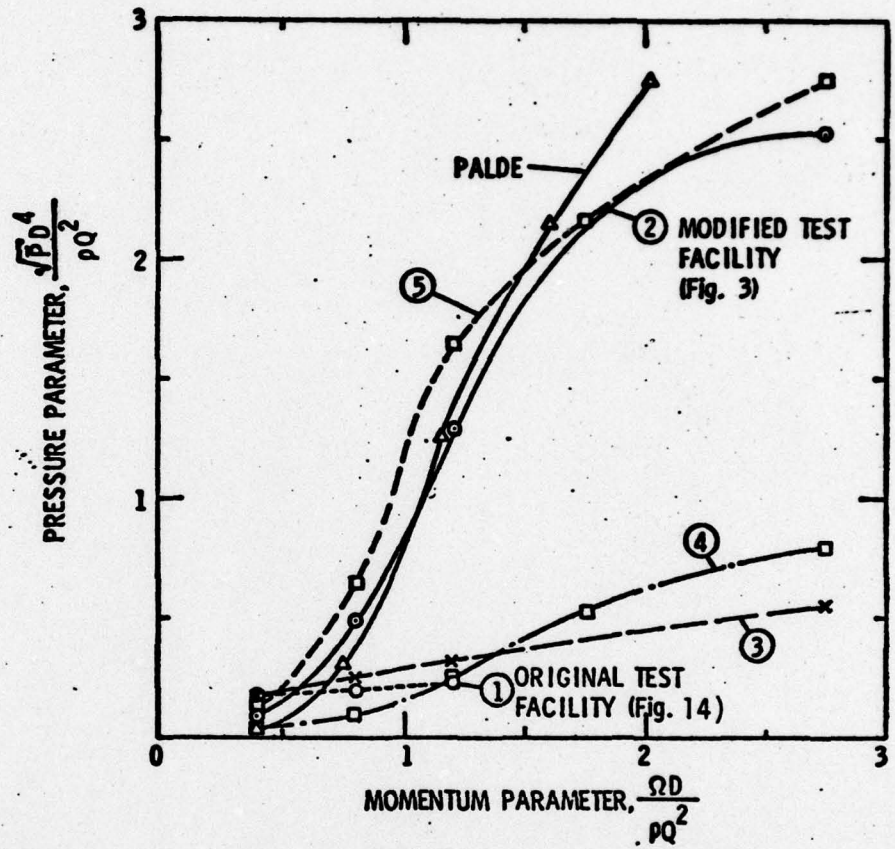


Figure A.2 - Pressure versus Momentum Parameter for the Cylindrical Draft Tube as a Function of Test Facility Geometry

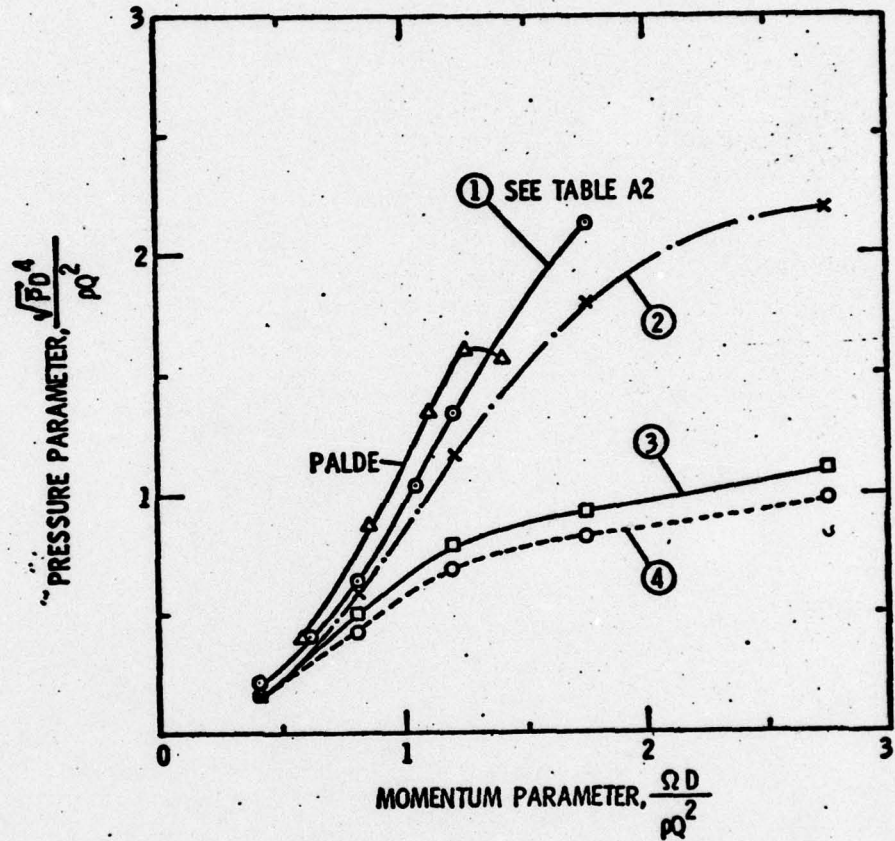


Figure A.3 - Pressure versus Momentum Parameter for the Fontenelle (Elbow Type) Draft Tube as a Function of Test Facility Geometry

DISTRIBUTION LIST FOR UNCLASSIFIED TM 78-56 by W. S. Gearhart, A. M. Yocum,  
and T. Seybert, dated 20 March 1978

Commander  
Naval Sea Systems Command  
Department of the Navy  
Washington, DC 20362  
Attn: Library  
Code NSEA-09G32  
(Copy Nos. 1 and 2)

Naval Sea Systems Command  
Attn: S. R. Marcus  
Code NSEA-03B  
(Copy No. 3)

Naval Sea Systems Command  
Attn: T. E. Peirce  
Code NSEA-0351  
(Copy No. 4)

Naval Sea Systems Command  
Attn: Code PMS-402  
(Copy No. 5)

Naval Sea Systems Command  
Attn: C. Miller  
Code NSEA-0331  
(Copy No. 6)

Naval Sea Systems Command  
Attn: A. R. Paladino  
Code NSEA-0372  
(Copy No. 7)

Naval Sea Systems Command  
Attn: C. G. McGuigan  
Code NSEA-03133  
(Copy No. 8)

Commander  
Naval Ship Engineering Center  
Department of the Navy  
Washington, DC 20362  
Attn: D. Burke  
Code NSEC-6140B.1  
(Copy No. 9)

Commanding Officer  
Naval Underwater Systems Center  
Newport, RI 02840  
Attn: Library  
Code LA15  
(Copy No. 10)

Commanding Officer  
Naval Ocean Systems Center  
San Diego, CA 92152  
Attn: J. W. Hoyt  
Code 2501  
(Copy No. 11)

Naval Ocean Systems Center  
Attn: T. Lang  
(Copy No. 12)

Commander  
David W. Taylor Naval Ship R&D Center  
Department of the Navy  
Bethesda, MD 20084  
Attn: W. B. Morgan  
Code 154  
(Copy No. 13)

David W. Taylor Naval Ship R&D Center  
Attn: R. Cumming  
Code 1544  
(Copy No. 14)

David W. Taylor Naval Ship R&D Center  
Attn: J. McCarthy  
Code 1552  
(Copy No. 15)

David W. Taylor Naval Ship R&D Center  
Attn: M. Sevik  
Code 19  
(Copy No. 16)

David W. Taylor Naval Ship R&D Center  
Attn: B. Cox  
Code 1544  
(Copy No. 17)

DISTRIBUTION LIST FOR UNCLASSIFIED TM 78-56 by W. S. Gearhart, A. M. Yocum,  
and T. Seybert, dated 20 March 1978 (continued)

David W. Taylor Naval Ship R&D Center  
Attn: J. L. Gore  
Code 1140  
(Copy No. 18)

Officer-in-Charge  
Annapolis Laboratory  
David W. Taylor Naval Ship R&D Center  
Department of the Navy  
Annapolis, MD 21402  
Attn: J. G. Stricker  
Code 2721  
(Copy No. 19)

David W. Taylor Naval Ship R&D Center  
Attn: Dr. E. R. Quandt, Jr.  
Code 272  
(Copy No. 20)

Commander  
Naval Surface Weapon Center  
Silver Spring, MD 20910  
Attn: Library  
(Copy No. 21)

Office of Naval Research  
Department of the Navy  
800 N. Quincy Street  
Arlington, VA 22217  
(Copy No. 22)

Defense Documentation Center  
5010 Duke Street  
Cameron Station  
Alexandria, VA 22314  
(Copy Nos. 23-34)

Mr. George Wong  
Rocketdyne Div. Rockwell Int.  
6633 Canoga Avenue  
Canoga Park, CA 91304  
(Copy No. 35)

NASA Lewis Research Center  
21000 Brookpark Road  
Cleveland, OH 44135  
Attn: N. Sanger  
(Copy No. 36)

Dr. G. K. Serovy  
Mechanical Engineering Department  
Iowa State University  
Ames, Iowa 50010  
(Copy No. 37)

Prof. J. Horlock  
Vice Chancellor  
University of Salford  
Salford, M5 4WT  
ENGLAND  
(Copy No. 38)

Dr. P. van Oossanen  
Netherlands Ship Model Basin  
Haagsteeg 2  
P. O. Box 28  
Wageningen  
THE NETHERLANDS  
(Copy No. 39)

Sir William Hawthorne  
Whittle Turbomachinery Laboratory  
Maddingley Road  
Cambridge  
ENGLAND  
(Copy No. 40)

Whittle Turbomachinery Laboratory  
Attn: Library  
(Copy No. 41)

Admiralty Marine Technology Establishment  
Teddington, Middlesex  
ENGLAND  
Attn: Dr. J. Foxwell  
(Copy No. 42)

Admiralty Marine Tech. Establishment  
Attn: Dr. A. Moore  
(Copy No. 43)

DISTRIBUTION LIST FOR UNCLASSIFIED TM 78-56 by W. S. Gearhart, A. M. Yocum,  
and T. Seybert, dated 20 March 1978 (continued)

Mr. Ken Ichirru  
Hitachi Ltd.  
4026 Kuji-cho  
Hitachi-shi  
Ibaraki-Ken, 319-12  
JAPAN  
(Copy No. 44)

Mr. Takashi Kubota  
Manager  
Hydro-Turbine Development  
Funi Electric Co., Ltd.  
1-1 Tanabeshinden,  
Kawasaki-ku  
Kawasaki City 210,  
JAPAN  
(Copy No. 45)

Mr. E. M. Greitzer  
MS-16 United Technologies  
Research Center  
Silver Lane  
E. Hartford, Connecticut 06118  
(Copy No. 46)

Mr. W. Whippen  
Allis-Chalmers  
Box 712  
York, PA 17405  
(Copy No. 47)

Mr. W. Swift  
Creare Inc.  
Box 71  
Hanover, NH 03755  
(Copy No. 48)

Mr. J. Lewis  
University of Newcastle  
Newcastle  
ENGLAND  
(Copy No. 49)

NASA Lewis Research Center  
21000 Brookpark Road  
Cleveland, Ohio 44135  
Attn: M. Hartmann  
(Copy No. 50)

Mr. R. K. Fisher, Jr.  
Allis-Chalmers  
Box 712  
York, PA 17405  
(Copy No. 51)

Dr. R. E. Henderson  
The Pennsylvania State University  
APPLIED RESEARCH LABORATORY  
Post Office Box 30  
State College, PA 16801  
(Copy No. 52)

GTWT Library  
The Pennsylvania State University  
APPLIED RESEARCH LABORATORY  
Post Office Box 30  
State College, PA 16801  
(Copy No. 53)

Mr. A. M. Yocum  
The Pennsylvania State University  
APPLIED RESEARCH LABORATORY  
Post Office Box 30  
State College, PA 16801  
(Copy No. 54)

Mr. W. S. Gearhart  
The Pennsylvania State University  
APPLIED RESEARCH LABORATORY  
Post Office Box 30  
State College, PA 16801  
(Copy No. 55)